Divergent consensus on the influence of Arctic Amplification on mid-latitude severe winter weather

J. Cohen[1,2], X. Zhang[3], J. Francis[4], T. Jung[5], R. Kwok[6], J. Overland[7], T. Ballinger[8], U.S. Bhatt[3], H. W. Chen[9], D. Coumou[10,11], S. Feldstein[9], D. Handorf[5], G. Henderson[12], M. Ionita[5], M. Kretschmer[10], F. Laliberte[13], S. Lee[9], H. W. Linderholm[14], W. Maslowski[15], Y. Peings[16], K. Pfeiffer[1], I. Rigor[17], T. Semmler[5], J. Stroeve[18], P.C. Taylor[19], S. Vavrus[20], T. Vihma[21], S. Wang[22], M. Wendisch[23], Y. Wu[24], J. Yoon[25]

[1]Atmospheric and Environmental Research, Inc. [2]Massachusetts Institute of Technology. [3]University of Alaska Fairbanks. [4]Rutgers University. [5]Alfred Wegener Institute Helmholtz Centre for Polar and Marine Research. [6]Jet Propulsion Laboratory. [7]NOAA/PMEL. [8]Department of Geography, Texas State University. [9]Pennsylvania State University. [10]Potsdam Institute for Climate Impact Research. [11]VU Amsterdam. [12]United States Naval Academy. [13]Environment and Climate Change Canada. [14]University of Gothenburg. [15]Naval Postgraduate School. [16]University of California, Irvine. [17]University of Washington. [18]University College London. [19]NASA Langley Research Center. [20]University of Wisconsin, Madison. [21]Finnish Meteorological Institute. [22]Utah Climate Center/Dept. PSC/Utah State Univ. [23]University of Leipzig. [24]Lamont-Doherty Earth Observatory, Columbia University. [25]Gwangju Institute of Science and Technology.

The Arctic has warmed more than twice as fast as the global average since the late 20th century, a phenomenon known as Arctic amplification (AA). It remains an open question whether amplified Arctic warming is influencing mid-latitude weather. Recently, there has been a significant advance in understanding the contributions to AA, which include melting sea ice; increased downward longwave radiation due to greater water vapor concentrations from local and remote sources; increasing ocean heat content; local and hemispheric atmospheric circulation changes; modified poleward heat transport in the atmosphere and ocean; and cloud radiative forcing. Also, since previous reviews on the topic (Vihma 2014; Cohen et al. 2014; Overland et al. 2015), progress has been made in understanding the different mechanisms linking AA to changes in mid-latitude weather. The pathway to

increased weather extremes considered most robust is reduced Barents-Kara Sea ice resulting in more frequent atmospheric blocking related to the Siberian and/or Ural high pressure system. Observational studies further suggest that this leads to a weakening of the polar vortex followed by increased severe winter weather across the mid-latitudes. Though some model experiments support the observational studies, other modeling experiments show little connection between AA and mid-latitude weather or suggest the export of excess heating from the Arctic to lower latitudes.

There is convincing scientific evidence that the Earth is warming as a result of increasing greenhouse gas concentrations from anthropogenic activities (IPCC 2013). The Arctic region exhibits amplified signs of this warming, particularly the rapidly declining sea ice extent in summer and early fall (Stroeve et al. 2012) in response to a variety of positive feedbacks (Pithan and Mauritsen, 2014; Döscher et al. 2014). A decrease in sea ice both reduces the surface albedo and increases the surface temperature, which results in larger latent and sensible heat fluxes into the atmosphere, further resulting in higher near-surface air temperatures and moistening of the Arctic boundary layer (Wendisch et al. 2017).

Coincident with AA has been an observed increase in extreme weather (Rahmstorf and Coumou 2011; Munich Re 2012; Cohen et al. 2014). A recent topic of scientific inquiry and debate is whether the increased extreme weather and AA may be physically linked. Because of the disruptive and costly impacts on society and ecosystems of extreme weather events, this potential linkage has garnered a great deal of interest by the media, public, business leaders and policymakers.

Over a decade ago it was proposed that Arctic warming (post 1988) and associated changes in

boundary forcing, including Arctic sea ice melt and increasing snow cover extent, influence mid-latitude weather via a stratospheric pathway resulting in cold temperatures across the mid-latitudes (Cohen and Barlow 2005). The pattern of a warm Arctic Ocean coupled with relatively cold temperatures across northern Asia, northern Europe and east of the Rocky Mountains in North America but focused in the Eastern US is known as the warm Arctic/cold continents pattern (Overland et al. 2011; Cohen et al. 2013). It was argued that the pattern of widespread warming in the fall coupled with regional cooling in Siberia is favorable for exciting vertical energy transport into the polar stratosphere resulting in a significant disruption of the stratospheric polar vortex followed by colder temperatures across the mid-latitudes in winter. This mechanism was in large part responsible for the observed winter cooling trends across the mid-latitude continents for the twenty years from 1989-2008 (Cohen et al. 2009). A composite of the temperature anomalies of the ten winters since that analysis shows nearly the same pattern of variability as for the previous temperature trends, suggesting that the same physical mechanism is responsible for the warm Arctic/cold continents pattern observed from 1989-2008 and 2009-2018 (**Supplementary Figure 1**).

Time series of winter temperatures for the Arctic and the mid-latitude continents from 1960-2018 illustrate AA (**Supplementary Figure 2)**. The difference between Arctic and mid-latitude land temperature anomalies was either negative or close to zero. Starting in 1988, Arctic temperatures began an almost monotonic warming trend that continues to the present and defines the period of AA. The warming further accelerated following the record minimum of sea ice extent of September 2007. In contrast, mid-latitude eastern continental land temperatures in winter have exhibited almost no warming over the same period and actually cooled from 2000-2013 followed

by warming in recent winters. The cooling is especially pronounced over northern Eurasia. Therefore the difference between Arctic and mid-latitude land temperature anomalies also exhibited a nearly monotonic increasing trend closely tracking Arctic temperature anomalies, with the winter of 2017/18 exhibiting the largest Arctic-mid-latitude positive difference on record (**Supplementary Figure 2)**. The increasing positive difference between Arctic and mid-latitude land temperature anomalies most pronounced in the cold season is a manifestation of AA.

The absence of a warming trend and in many locations a winter cooling trend across the mid-latitude continents for most of the twenty-first century came as a surprise to climate scientists, as this result was not predicted by the models (Cohen et al. 2012a) and likely contributed to the global warming hiatus observed over the same period (Cohen et al. 2012b). This cooling trend was the strongest observational evidence that some unaccounted mechanism was offsetting greenhouse gas forced warming. Theories included internal variability and tropical forcing but also a new idea—AA contributed to mid-latitude cooling. However as we will discuss in this review, a range of results exist in both observational and modeling studies; though some modeling results can match the observed changes, other modeling studies demonstrate the opposite. Furthermore, the recent rise in mid-latitude winter warming is suggestive that the cooling seen over the past thirty years could be oscillatory and therefore attributable to natural variability. Still, Eurasian winter cooling was detected also during the previous period of AA in 1930s-1940s (Wegmann et al. 2017), which may suggest a forced response to AA.

The recent mid-latitude winter cooling period has coincided with an increase in extreme winter weather (Cohen et al. 2014, 2018a). Anticipating extreme weather can save lives and prevent or

mitigate economic losses. Furthermore, the occurrence of severe winter weather also tends to fan skepticism that climate change is occurring and can act as an impediment to implementing policies to mitigation and adaptation to climate change, highlighting the societal need to understand the underlying physical pathways correctly. **Supplementary Figure 2** illustrates the plausibility of attributing mid-latitude continental cooling to AA but the challenge of demonstrating such a linkage is daunting using different observational analysis combined with large numerical model spread. Simple causality statements for a general audience have not been forthcoming.

The character of Arctic amplification

In recent decades, the Arctic has undergone substantial change that in many cases has been rapid and unprecedented (Taylor et al. 2017). AA is defined by its characteristic surface-based warming profile, where Arctic surface and low troposphere air temperatures have warmed more than twice as fast as the global average temperature and this warming trend has increased to more than six times of global mean during the most recent decade (Huang et al. 2017). The enhanced sensitivity of the Arctic has been known for some time from modeling experiments (Manabe and Wetherald 1975; Alexeev 2005). Moreover, AA is focused in fall and winter months and is mostly absent in summer.

Figure 1 shows Northern Hemisphere and Arctic zonal mean winter air temperature trends between 1981-2015 from the surface to upper atmosphere. The air temperatures were averaged in four reanalysis datasets. Reanalysis datasets are created by numerical models assimilating observed data collected from various platforms and provide a best estimate of the real world; in the remainder of the article, reanalysis datasets will be considered as "observations." Amplified Arctic warming is evident, with AA strongest during fall and winter and weakest during summer

(Cohen et al. 2018a). The vertical distribution of Arctic winter temperature trends shows a warming that extends throughout the troposphere and is strongest near the surface. However, there is a second warming maximum in the upper troposphere, which extends into the stratosphere. The winter warming polar stratosphere trend is evident in radiosonde data as well (Alexeev et al. 2012). Comparison with simulated Arctic warming from the Fifth Coupled Model Intercomparison Project (CMIP5) shows that the model ensemble mean lacks the observed magnitude of the surface-based warming, the vertical extent of the warming and the observed warming in the upper troposphere and stratosphere is completely absent (**Figure 1)**. The shallower warming in models is consistent with previous studies, showing that models simulate too strong an Arctic temperature inversion (Boe et al. 2009), which would inhibit the vertical distribution of surface warming. This model deficiency may be in part due to coarse vertical resolution (Vihma 2017).

Besides coupled models, we also analyzed the vertical distribution of temperature trends in models forced with observed sea surface temperatures (SSTs) and sea ice from the Atmospheric Model Intercomparison Project (AMIP). The results are similar to those of CMIP5 with relatively shallow Arctic warming and the secondary warming maximum in the stratosphere mostly absent (**Figure 1** and **Supplementary Figure 3**). Further analysis of individual ensemble members reveals that several members closely match the distribution of observed hemispheric temperature trends with a deeper warming in the Arctic in the lower to mid-troposphere and a secondary warming maximum in the stratosphere (**Supplementary Figure 4**); the best individual ensemble member match to the reanalysis data is included in **Figure 1**. This suite of model runs suggests that differences between the model ensemble mean and observations could be due to natural variability, which is averaged out in the large ensemble mean of model simulations. Furthermore at least some model members are able to simulate the observed trend. Therefore the large ensemble mean of

multi-model simulations support that the observed trends are not a forced response but rather a result of natural variability.

Arctic amplification mechanisms

Understanding of the mechanisms contributing to amplified Arctic warming has significantly evolved in the last decade, emphasizing that a suite of mechanisms are responsible for the enhanced sensitivity of the Arctic. These mechanisms causing AA can be divided into local and remote forcings. The local forcings include sea ice-albedo, surface heating and ice insulation feedbacks, which are typically considered the trigger in the causal chain leading to AA (Stroeve et al. 2012). Remote forcing mechanisms involve heat and moisture transport from the mid-latitudes and tropics into the Arctic, which can be reinforced by the positive phase of the Arctic Oscillation (AO) circulation pattern (Rigor et al. 2002; Zhang et al. 2003). Recent studies further argue that remote mechanisms are more important contributors to the observed amplification of Arctic warming and acceleration in sea ice disappearance during both winter (Zhang et al. 2008, 2013; D.-S. Park et al. 2015a; Gong et al. 2017) and summer (Zhang et al. 2008; Zhang et al. 2013; Laliberté and Kushner 2014; Ding et al. 2017). Local and remote mechanisms may also interact and can amplify one another. For instance, tropical convection-forced warming through the transport of heat and moisture may be further amplified by local feedback processes, e.g., increasing heat trapping clouds. The range of processes contributed to AA are summarized in **Figure 2**.

Perhaps the best-known Arctic feedback is the sea ice albedo feedback (Perovich et al. 2008), owing its existence to the stark albedo difference between ice-free ocean and snow-covered sea ice surfaces (cf. ~7% with ~80% reflectance, respectively). The darkening the Arctic surface has been observationally confirmed indicating an Arctic surface albedo reduction from 0.52 to 0.48 since 1979 (Pistone et al. 2014). The increase in vegetation over Arctic land also contributes to a

darkening surface at high latitudes (Jeong et al. 2014). Additionally, rapid spring snow cover loss lowers the albedo and allows the underlying soil to dry out earlier, favoring earlier and more intense warming of high-latitude land areas (Overland et al. 2012).

During winter, insulation by sea ice decouples the ocean from the atmosphere, preventing the moderation of Arctic air masses by latent and sensible heat fluxes from the Arctic Ocean; an insulating process that is waning in the period of AA. For example, anomalously low sea ice extent during the summer exposes darker (i.e., low albedo) ocean water to sunlight, producing Arctic warming via absorption of solar radiation in the upper ocean mixing layer promoting anomalous latent and sensible heat fluxes in the fall. Subsequently, this process delays fall/winter sea ice re-growth allowing for warmer and moister Arctic air masses, further contributing to AA (e.g., Serreze and Francis 2006; Screen and Simmonds 2010). Analysis of surface turbulent flux trends indicate enhanced fluxes from the ocean to the atmosphere in the Chukchi and Kara Seas in recent years (Screen and Simmonds 2010; Boisvert et al. 2015; Boisvert and Stroeve 2015; Taylor et al. 2018).

A new consideration of equal, or possibly more importance, is local feedback related to the impact of low-level mixed-phase clouds on the surface energy budget. Arctic clouds warm the surface via enhanced downward terrestrial, longwave radiation for much of the year (predominantly during the polar night in winter), except in June and July when the reflection of solar radiation by clouds dominates, cooling the surface (Kay and L'Ecuyer 2013; Boeke and Taylor 2016). The impact of clouds is further complicated by the seasonal evolution of surface albedo, including the summer sea ice melt and production of melt ponds (Intrieri et al. 2002). Results from CMIP5 models disagree about whether Arctic cloud changes dampen or amplify AA (Pithan and Mauritsen 2014; Boeke and Taylor 2018).

187 The importance of downward longwave radiation on AA and sea ice has been identified by a
188 number of studies (Uttal et al. 2002; Francis et al. 2005; Screen 2017a). With respect to sea ice
189 cover, emerging evidence suggests that anomalous cloud cover and downward longwave radiation
190 during winter can hinder sea ice growth (Liu and Key 2014; Lee 2014; H.-S. Park et al. 2015b;
191 Hegyi and Taylor 2017). Analysis of CMIP5 models indicate that changes in the downward clear-
192 sky longwave flux from the atmosphere, rather than the surface albedo feedback, is the largest
193 contributing factor to simulated AA (Boeke and Taylor 2018). Observations indicate that trends in
194 downward longwave radiation are positive almost everywhere over the Arctic Ocean for all
195 seasons (Cohen et al. 2018a). Additional discussion on AA mechanisms is included in the
196 Supplementary Information (SI).

197 Despite the robust signal of AA, knowledge of the mechanisms remains incomplete. We are just
198 beginning to understand the role of atmospheric heat transport and, particularly, the importance of
199 the episodic deposition of heat and moisture at the synoptic scale. However, a more comprehensive
200 understanding of the chain of events leading to AA and the individual process contributions is
201 needed, as the magnitude and mechanisms of AA fundamentally influence the character and
202 likelihood of Arctic and mid-latitude connections.

203 **Arctic mid-latitude linkages including extreme events**

204 There is a greater thermodynamic connection of the Arctic Ocean with the overlying atmosphere
205 in the cold months over extensive new sea ice-free areas in autumn and thinner sea ice in early
206 winter months allowing for greater heating of the overlying atmosphere. Enhanced surface
207 turbulent heat fluxes from the surface to the atmosphere due to reduced sea ice cover represent a
208 possible mechanism linking AA to mid-latitude weather. Preferential warming of the atmospheric
209 column leads to increased geopotential height thickness and a reduced meridional gradient of the

geopotential heights as described by the geopotential tendency equation (Holton 1979), which can slow the Jet Stream. It has been theorized that this further increases the amplitudes of the Rossby waves, decrease their phase speed, and enhance the possibility of blocking situations (Francis and Varus 2012).

A research challenge is to detect possible links from thermal heating from Arctic sources to mid-latitude weather. Amplified Arctic warming does increase the potential for Arctic change to influence weather outside of the Arctic. However, mid-latitude weather is also strongly steered by highly nonlinear jet stream dynamics and anomalous mid-latitude and tropical SST forcing. Arctic-mid-latitude linkages may also be background state-dependent, i.e., linkages may be more favorable in one atmospheric wave pattern than another, creating intermittency (Overland et al. 2016) and/or masked by internal variability (Shepherd 2016). The impact of anomalous transient storm systems on the growth and phasing of planetary waves, the onset and maintenance of blocking, and the strength and location of the Siberian High may be preconditioned by the state of the hemispheric atmospheric background flow (Overland et al. 2016).

Understanding Arctic and mid-latitude linkages is societally-relevant and complex, adding to the controversial nature of the topic, especially the possible link to extreme weather (Wallace et al. 2014; Kintisch 2014; Gramling 2015). Although the term *extreme weather* is used to describe a range of phenomena, their common trait is the potential for high socioeconomic impact. Such events can be either short-lived (e.g., hurricane or blizzard), or persistent for weeks, months or longer (e.g., droughts and floods). It is expected that a warming globe will lead to an overall increase in extreme weather, especially heat and heavy precipitation extremes but decreases in cold extremes based upon thermodynamic considerations and model simulations (Coumou and Rahmstorf 2012; Cohen et al. 2014; Melilo et al. 2014; Lehman et al. 2015; Diffenbaugh et al.

2017; Johnson et al. 2018). Longer term trends show a decrease in cold extremes as projected by the models, however unexpectedly during the era of AA, cold extremes have exhibited an increasing trend (Cohen et al. 2014; Johnson et al. 2018). In addition, heavy snowfall events have increased over the past decade in the Northeastern US (**Supplementary Figure 5**).

Changes in the magnitude and frequency of severe winter weather has important implications for society, disrupting transportation, lowering economic productivity and even leading to loss of life. A lack of understanding of dynamics and feedback mechanisms driving variability in weather extremes and subsequent model deficiencies contribute to poor predictions of extreme weather events (Christensen et al. 2008; Min et al. 2013). Yet, the projected change in frequency and intensity of extreme weather events is considered one of the most consequential yet more poorly understood impacts of climate change (Sillmann et al. 2013; NAS 2016) with the known variability in linkage processes limiting straight-forward cause and effect predictions..

Atmospheric blocking events play a key role in many extreme weather events (Coumou and Rahmstorf 2012). Blocking patterns result from the breakdown of the background flow pattern, which makes weather systems move slower or even become stationary (Rex 1950a,b). Like boulders blocking a river, once an atmospheric block forms, its impacts are felt both upstream and downstream of the block. Extreme cold temperatures during the winter months over Europe and North America are associated with blocking anticyclones over northwestern Eurasia high latitudes and Greenland, respectively (e.g., Thompson and Wallace 2001; Honda et al. 2009; Sillmann et al. 2011; Francis and Vavrus 2012; Zhang et al. 2012; Cohen et al. 2018b; Johnson et al. 2018). Moreover, blocking events have been implicated as precursors for sudden stratospheric warmings (Quiroz 1979, 1986; Martius et. al. 2009), which in turn influence surface weather evolution for up to two months later during winter (Baldwin and Dunkerton 2001; Kim et al. 2014; Kretschmer

et al. 2018). Theories linking the AA to severe or extreme winter weather including the role of blocking are discussed below.

Hemispheric wide response of AA

The surface warming over the Arctic Ocean during the delayed re-freezing in autumn—along with increased surface turbulent heat fluxes and reduced vertical stability—can fuel intense storm systems over the Arctic (Jaiser et al. 2012; Semmler et al. 2016; Basu et al. 2018). The non-linear interaction between storm systems and planetary-scale waves contributes to changes in atmospheric circulation, which can constructively or destructively interfere with the large climatological standing waves; enhancement (destruction) of these waves can increase (decrease) upward propagation of energy in early- to mid-winter to weaken (strengthen) the stratospheric polar vortex (Smith et al. 2011). The tropospheric response to either a weakening or strengthening polar vortex is hemispheric in scale and most closely resembles the negative or positive AO, respectively (Cohen et al. 2007, 2014).

Consistent with these ideas, many of the early studies on the relationship between Arctic sea ice and mid-latitude weather presented the physical connection in terms of Arctic sea ice extent anomalies forcing a hemispheric-wide atmospheric response most often related with the AO pattern of variability (Cohen et al. 2014). The earliest modeling studies demonstrated that complete Arctic sea ice melt influenced mid-latitude weather that was consistent with the negative AO phase (Newson 1973; Warshaw and Rapp 1973). Later modeling studies found that reduced sea ice extent regionally, predominately forced an atmospheric response that also closely resembles the negative phase of the AO with increased sea level pressure (SLP) over the Arctic and decreased SLP over the mid-latitudes in winter (Magnusdottir et al. 2004; Deser et al. 2004; Alexander et al. 2004).

Another early numerical study forced the Hadley Centre Atmosphere-3 (HadAM3) global climate model (GCM) with sea ice variability and found no significant relationship between differences in sea-ice concentration and the AO (Singarayer et al. 2005). Many more large ensemble modeling studies came to the same conclusion about a decade later—there is little modeling evidence of a significant atmospheric response to sea ice variability (e.g., McCusker et al. 2016; Blackport and Kushner 2017; Ogawa et al. 2018).

Regional response of AA

While previous review articles on the influence of AA on mid-latitude weather have focused on the hemispheric response projected onto the AO pattern of variability (Vihma 2014; Cohen et al. 2014; Overland et al. 2015), it is becoming better understood that regional anomalies in sea ice or temperature can force regional responses in mid-latitude weather. Most studies have focused on the relationship between sea ice loss and/or warming in the Barents-Kara Seas region with cold temperatures across Asia and Siberia for the recent period (Mori et al. 2014) and even during the early twentieth century (Wegmann et al. 2017). However there have been a few studies also suggesting a link between sea ice melt and/or warming over the Chukchi Sea and central North American cold temperatures (Kug et al. 2015) and sea ice melt and/or warming in and around Greenland and eastern North American and Northern European temperatures (Chen and Luo 2017). Additional detail on the regional response to AA is provided in the SI.

Though there is a range of results between observational and modeling studies on the hemispheric response to sea ice loss, there is some agreement on the downstream regional response to regional Arctic sea ice loss and/or warming. Analysis of recent Arctic sea ice concentration trends shows three main regions of sea ice retreat: Barents-Kara Seas, Chukchi-Bering Seas and around Greenland (see **Supplementary Figure 6**). In **Figure 3**, we plot the temperature anomalies

associated with above to well above normal winter temperatures in the Barents-Kara, Baffin, Greenland and Chukchi-Bering Seas, respectively, in both the observations and from the Hadley Centre Global Environmental Model-2 (HadGEM2). Regional warming in the Barents-Kara Seas is linked to below normal temperatures across Central and East Asia. Regional warming in the Baffin-Greenland Seas is associated with below normal temperatures across Northern and Central Europe and to a lesser degree eastern North America. Finally, regional warming in the Chukchi-Bering Seas is associated with below normal temperatures across Central and Eastern North America. Another study using observed regional sea ice extents found similar associations between anomalously low autumn sea ice in the Barents-Kara and Greenland Seas and lower winter temperatures over Eurasia (Chen et al. 2016a). Somewhat consistent results were found when the HadGEM2 was forced with regional sea ice loss (**Figure 3**; Screen 2017a). Sea ice loss in the Barents-Kara Seas resulted in weak cooling across Eurasia, sea ice loss in the Baffin and Greenland Seas resulted in cooling across Europe, parts of Canada and the Eastern US and sea ice loss in the Beaufort-Chukchi Seas resulted in cooling in parts of North America.

Besides forcing cold temperatures regionally, both models and observations may further agree that regional sea ice loss in the Barents-Kara Seas results in a weakened stratospheric polar vortex followed by a negative AO response (Kim et al. 2014; Sun et al. 2015; Screen 2017a; Zhang et al. 2018).

However, even though the regression of pan-Arctic warmth with hemispheric temperatures yields mid-latitude cooling in both the observations and the model, when the sea ice loss is pan-Arctic it no longer forces a weakened polar vortex in the models (Sun et al. 2015; Screen 2017a) and cooling across the mid-latitudes is nearly absent (**Figure 3**).

In general, the cooling from the modeling experiments is weaker than that derived from observational analysis. Also, while regional sea ice loss resulted in downstream localized cooling, pan-Arctic sea ice loss resulted in warming across the Arctic and adjacent land areas and in almost no discernable cooling (Screen 2017a). Overall, the model experiments mainly support the hypothesis that the warm Arctic/cold continent pattern is not forced by pan-Arctic sea ice loss and/or AA.

Observational analysis versus model data

Mostly derived from observational analysis, there have been several theories proposed on the mechanisms for how Arctic change influences mid-latitude weather, including changes to the Jet Stream, wave amplitude and speed, troposphere-stratosphere coupling and blocking (Cohen et al. 2018b). There has also been a wide spectrum of model responses to Arctic sea ice loss from no response to warming and cooling of the mid-latitudes. **Figure 4a** displays the observed temperature anomaly for the mid-latitude continents (all land points 30-60°N) of December through March from 1988/89 through 2017/18 from observations and the corresponding predicted temperature anomaly from the North American Multi Model Ensemble (NMME; Kirtman et al. 2014) initialized with atmospheric and oceanic conditions including sea ice on November 1 for each year. There exists a fairly wide scatter of predicted and observed temperature anomalies over the period with little sense of organization or forcing other than the temperature anomalies being skewed warm and could be considered representative of the noisy nature of mid-latitude weather and the lack of consensus of Arctic forcing of mid-latitude weather.

Next, in **Figure 4b**, we plot the reanalysis values in blue and the model forecast values in red, which reveals some systematic patterns. The observed temperature anomalies are either on the cold extreme of the envelope of model forecasts and in many winters are even colder than the most

extreme cold ensemble member. In **Figure 4c**, the reanalysis values are plotted with the ensemble mean of the model forecasts only and a clear dichotomy appears—the observed value is always colder than the ensemble mean in the era of AA without exception. Also included is the trend line for both the observed and predicted winter temperature anomalies. The trend lines are clearly diverging with the model predicted temperatures exhibiting accelerated warming relative to the observed temperatures.

Finally, in **Figure 4d** Northern Hemisphere (NH) land and ocean temperatures are included for both the observations and the model forecasts including the trend line. Despite the clear divergence in mid-latitude land winter temperatures, there is good agreement between the model-predicted and observed hemispheric winter temperatures with comparable warming in both the observed and simulated temperatures.

Figure 4 represents a new paradigm of two distinct and divergent camps on the influence of AA on mid-latitude weather. Though the NH is warming in the GCMs at a rate comparable to the observed warming, the distribution of that heat is clearly different in the era of AA, at least through the present. The models suggest that during AA, anomalous heating is more equitably distributed between the Arctic and the mid-latitudes so that both regions are warming at a rate comparable or faster than the hemispheric average. Based on previous observational studies which argue that AA is forcing continental cooling, the reanalysis suggests the counter-intuitive idea that accelerated Arctic warming favors the further import of heat into the Arctic from the mid-latitudes, resulting in the NH mid-latitudes continents cooling relative to the remainder of the hemisphere with further accelerated Arctic warming.

During the period of AA, the observations show that temperatures across the mid-latitude continents have remained nearly constant. In contrast, the models predict that the mid-latitudes

should be warming at a rate nearly identical to the warming for the entire NH of +0.038°C/year. In **Supplementary Figure 7**, the mid-latitude oceans, tropics and the Arctic time series are plotted for both the observations and the NMME ensemble. The simulated warming is nearly identical to the observed warming in the tropics and mid-latitude oceans. However, the simulated warming in the Arctic is only half of that observed. This is in contrast to the continental mid-latitudes where the model warming is accelerated relative to the observed—the model simulated warming of the mid-latitude continents is diverging from the observed rate by about +0.36°C/year.

To what scientists attribute the divergence between observed and simulated temperatures trends likely depends on the research tool employed. Based on empirical studies, AA is resulting in a mid-latitude cooling of approximately -0.05°C/year relative to the remainder of the NH. Based on modeling studies, the NH mid-latitude continents should be warming at a rate comparable or slightly higher than the remainder of the NH. The divergence in simulated and observed trends can be explained by natural variability.

There is a clear cold bias in the NMME models compared to the observations (**Supplementary Figure 8**), however all arguments are based on the trends which are insensitive to climatology and not the sign or magnitude of the temperature anomalies.

The model simulated high-latitude amplified warming is relatively shallow but horizontally expansive (**Figure 1**). The model simulated warming is favorable for a weak but not amplified disruption of the polar vortex. In contrast, empirical studies have highlighted that the excessive Arctic heat is distributed vertically through the lower and mid-troposphere and not horizontally (**Figure 1**). The vertical distribution of the heat in the Arctic that extends to the mid-troposphere supports high latitude blocking that further favors a convergence of heat in the polar stratosphere transported from lower latitudes that leads to a more amplified disrupted polar vortex. Robust

polar vortex disruptions displace Arctic air further south into the mid-latitudes resulting in, if not a cooling of the mid-latitudes, at least a delay in the warming rate of the mid-latitude continents relative to the remainder of the NH. A simplified explanation of the warm Arctic/cold continents pattern in the era of AA based on the majority of observational analysis and model data is provided in **Boxes 1** and **2**, respectively.

Conclusions

Improved understanding of Arctic forcing of mid-latitude weather linkages, combined with internal variability and equatorial and mid-latitude SST forcing, provide a clear pathway forward for improving subseasonal to seasonal weather outlooks and will aid policy makers in decisions and activities related to climate change. Projections have been for winters to become increasingly mild with less frequent snowfalls. However, severe winter weather persists and in some regions heavy snowfalls have become more, not less, frequent (Cohen et al. 2018b). Though there are a growing number of studies argue that AA has contributed to more frequent severe winter weather there area also a growing number of studies argue that the influence of basin-wide Arctic change on mid-latitude weather is either insignificant or contributing to milder winters. The divergence of studies and opinions has made the topic of Arctic influence on mid-latitude weather controversial and the field has been described as one with a lack of consensus (Wallace et al. 2014; Kintisch 2014; Gramling 2015). An alternate interpretation based on the large number of studies from the last few years is that there is simply a wide range of results based on the complexity and intermittency of Arctic/midlatitude connections.

In this review, we show advances from surveying the observational and numerical. First, we highlight that AA is not limited to sea ice melt but has multiple causes and is still an unsettled

issue. We then discuss whether AA influences mid-latitude weather or not. The topic could be described or symbolized by scatter and lack of consensus, such scatter can be considered as part of natural processes. However a closer look reveals a clustering of scientific evidence and ideas. Regionalization of sea ice anomalies and the atmospheric response are important and the models and observational studies may share common ground not fully appreciated. However, the influence of pan-Arctic change simulated in models and argued from observational analysis are clearly divergent with observational studies, arguing that AA forces cooling in the mid-latitudes while the majority of modeling experiments do not. The distribution of heating rates in the models closely aligns with expectations of AA, i.e., the warming increases with latitude, the tropics warm the least, the Arctic the most and the mid-latitudes are somewhere in between and close to the hemispheric average. The observed distribution of heating rates, where the mid-latitudes warm the least followed by the tropics and then greatly accelerates over the Arctic, likely cannot be explained without including dynamical arguments either forced by AA or simply due to natural variability.

Recognition of the warming asymmetry among empirical and modeling studies allows for discriminating dynamic mechanisms argued by both observational analysis and model data. A more vertically extensive heating of the atmosphere, characterized by the observations, favors more high latitude blocking and more frequent disruption of the polar vortex, followed by displacement of cold air normally residing in the Arctic to lower latitudes and increasing the episodes of severe winter weather. In contrast, the models simulate a shallower pan Arctic distribution of heat that does not significantly alter the behavior of the polar vortex and instead modifies the episodic discharge of Arctic air to mid-latitudes resulting in ever milder winters.

Therefore, thermodynamic warming overwhelms dynamic cooling in the mid-latitudes. Though, as discussed above, modeling studies with regional sea ice melt confined to the Barents-Kara Seas did produce a weakened polar vortex consistent with the observations. In addition to natural variability, some of the differences in observed and modeled polar vortex behavior may be due to the fact that most GCMs are "low-top" models and only poorly resolve the stratosphere and stratosphere-troposphere coupling mechanisms (Charlton-Perez et al. 2013). The increasing availability of high-top climate models with improved stratospheric variability should bring new insights on this discrepancy between observations and models (Sun et al. 2015). However, as shown by the range of ensemble member results for the same forcing conditions, natural variability may be the major factor.

Figure 4 provides a metric to measure consensus among models and observational studies. Currently, the observed and simulated NH mid-latitude continental temperature trends are diverging with simulated NH continental temperatures accelerating away from observed temperatures at a rate of 0.36°C/year. If future observed mid-latitude winters warm while converging towards simulated trends, then the current divergence was likely a result of natural variability or the inherent noise of the climate system. A set of coordinated modeling studies are planned (Smith et al. 2018) that are targeted to better quantify the forced response to sea ice loss. In those experiments, observations will be used to constrain the model response to sea ice loss (Screen et al. 2018) so that models and observations together provide a better estimate of the forced response.

Future understanding of the Arctic/midlatitude weather linkage may conclude that a robust intermittency of circulation pattern obfuscates a direct cause-and-effect of AA forcing. This may appear less than satisfactory in explaining such phenomenon to a general public, but it is closer to the current state of the science. Regardless, this survey of the literature provides an important step to a better understanding and eventual progress towards consensus of this scientific and societally important topic.

Box - B1 Observational studies:

It is now accepted that rapid Arctic change is contributing to recent changes in mid-latitude climate and weather, as well as the occurrence of extreme events. However, the question of how significant the contribution is, is it detectable and what mechanisms are responsible are less well understood. Observational studies have argued for a varied AO response to sea ice forcing, however over the past decade the observational studies have predominantly argued that low sea ice favors a negative AO and cold temperatures across the NH continents (Overland et al. 2016).

Based on the consideration of a large majority of observational analysis, we identified a list of proposed physical processes or mechanisms that may play an important role in linking Arctic change to mid-latitude climate and weather. The list, ordered from high to low confidence, includes: increasing geopotential thickness over the Arctic (Overland and Wang 2010; Cohen et al. 2018b); weakening of the thermal wind (Francis and Vavrus 2012); modulating stratosphere-troposphere coupling (Cohen et al. 2007; Kim et al. 2014; Zhang et al. 2018); exciting anomalous planetary waves or stationary Rossby waves in winter and modulating transient synoptic waves in summer (Honda et al. 2009; Coumou et al. 2015); changes in the atmospheric circulation and associated strengthening of the Siberian high and Aleutian low (Zhang et al. 2008; Blackport and Kushner 2017; Screen et al. 2018); altering storm tracks and behavior of blockings (Franics and Vavaru 2015; DiCapua and Coumou 2016; Basu et al. 2018); and increasing frequency of occurrence of summer wave resonance (Coumou et al. 2014). The dynamical pathway considered most robust is the diminished Barents-Kara sea ice, contributing to a northwestward expansion of the Siberian high or Ural blocking leading to cold Eurasian winters (Cohen et al. 2014).

The region of the Arctic that has seen the greatest area of sea ice loss is the Barents-Kara Seas (**Supplementary Figure 6**). This leads to heating of the overlying atmosphere, dilation of the geopotential heights and a weakening of the westerly wind resulting in increased blocking over the Barents-Kara Seas and adjacent Ural Mountains region (Yao et al. 2017). A ridge over northwestern Eurasia with a trough over northeastern Eurasia is favorable for the direct forcing of planetary waves with enhanced vertical propagation of wave energy into the stratosphere (Cohen et al. 2007; Nakamura et al. 2015). This can lead to wave breaking and disruption of the stratospheric polar vortex (Jaiser et al. 2016). Significant disruption of the polar vortex is then followed by widespread cold temperatures across the NH mid-latitude continents but with a focus across Asia (Kretschmer et al. 2018). Furthermore, a recent observational study showed that a weak polar vortex is related to more frequent heavy snowfalls in the Eastern US (Cohen et al. 2018b).

In **Figure B1** we summarize, based on the observational analysis, how AA in general and sea ice loss in particular can influence mid-latitude weather in winter via a stratospheric pathway. During the winter months, due to lack of solar radiation, cold air pools over the Arctic as milder air circulates at lower latitudes. Cold air is dense, causing a contraction of geopotential heights over the Arctic while mild air is light, causing a dilation of geopotential heights at lower latitudes. Low heights centered over the North Pole with heights rising in the direction of the equator favors the flow of air down gradient towards the North Pole, however the air is deflected to the east by the Coriolis force. The pooling of cold air over the shallower geopotential heights over the Arctic encircled by a fast flowing ribbon of westerly winds traps cold air near the Pole with milder air over the mid-latitudes and sub-tropics.

In recent decades this climatologically favored configuration of the polar vortex has become increasingly perturbed (Cohen et al. 2009; Kretschmer et al. 2018). Sea ice loss has warmed the Arctic region from below but based on **Figure 1** that heating is not confined to the near surface but rather extends through the mid-troposphere suggestive of a more active convective mechanism in distribution of the heat compared to the models. In addition, the sea ice loss is not uniform but rather focused in the Barents-Kara Seas. Dilation of geopotential heights from a warmer troposphere centered over the Barents-Kara Seas and northwestern Eurasia is favorable for excitation of vertically propagating energy excited by large-scale planetary waves. This additional energy is deposited in the polar stratosphere causing a second maxima of Arctic heating in the polar upper troposphere and stratosphere (**Figure 1)** where the polar vortex normally resides. Heating of the Arctic atmosphere from the ocean surface through the stratosphere dilates the atmosphere sufficiently to reverse the normally low geopotential heights to high geopotential heights surrounded by lower heights at more southerly latitudes. Now the down gradient is away from the North Pole and towards the equator and cold air previously trapped near the Pole is displaced to the mid-latitudes. As air flows away from the North Pole towards the equator, the air is deflected to the west, forming an easterly ribbon of air flowing around the North Pole. The more frequent displacement of cold air from the Arctic to the mid-latitudes has, if not cooled the mid-latitudes relative to earlier decades, at least offset some of the warming across the mid-latitude continents that has occurred more rapidly elsewhere across the NH.

Box – B2 Modeling data:

The earliest modeling studies found that pan-Arctic or low Arctic sea ice mainly east of Greenland and extending into the Barents-Kara seas forced a negative AO and cold temperatures across the NH continents (Newson 1973; Warshaw and Rapp 1973; Magnusdottir et al. 2004; Deser et al. 2004; Alexander et al. 2004). However since then, modeling studies have supported the entire range of atmospheric response from cold continents (Honda et al. 2009; Orsolini et al. 2012; Kim et al. 2014; Mori et al. 2014; Zhang et al. 2018) and the negative AO (Deser et al. 2015; Nakamura et al. 2015) to a positive AO (Screen et al. 2014; Smith et al. 2017) and mild continental temperatures (Ayarzagüena and Screen 2016) to no robust impact on mid-latitude weather (McCusker et al. 2016; Chen et al. 2016b; Blackport and Kushner 2017; Ogawa et al. 2018).

However, in the majority of modeling studies, especially the most recent ones where large ensembles are used, the atmospheric response is small relative to the internal variability and does not force cold winters across the NH mid-latitude continents (Sun et al 2016; McCusker et al. 2016; Chen et al. 2016b; Blackport and Kushner 2017; Smith et al. 2017; Ogawa et al. 2018). And in one study, even though regional Arctic sea ice loss forced downstream cooling across the continents locally and sea ice loss in the Barents-Kara Seas did result in weakened polar vortex, pan Arctic sea ice loss resulted in either no significant temperature change or significant warming across the continents (Screen 2017a). So even though models do simulate regional cooling from regional sea ice loss, the cumulative response does not add linearly but rather destructively interferes and results in overall warming across the continents.

555 Though there remains much uncertainty in the simulated dynamical response to Arctic sea ice loss
556 (Screen et al. 2018), based on the trend in the most recent large ensemble modeling studies and
557 analysis from CMIP5 and AMIP ensembles (**Figure 1 and Supplementary Figure 3**) and the
558 NMME ensembles (**Figure 4**), the atmospheric response in the mid-latitudes to pan Arctic sea ice
559 loss can be summarized as either small to be almost insignificant or resulting in further warming
560 of the mid-latitude continents in addition to radiative forced warming.
561
562 Comparing the horizontal and vertical extent of the warming in boreal winter shows that the
563 simulated warming is horizontally more extensive in the CMIP5 and AMIP models compared to
564 the observations (**Figure 1**). Whereas the Arctic warming is greater in the observations, it is also
565 more geographically limited with the amplified warming of the high latitudes extending further
566 south in the models. This result is consistent with a previous study where it was argued that the
567 more extensive simulated warming is due to the horizontal distribution of heat via advection or
568 conduction from the Arctic to lower latitdues(Cohen et al. 2013).
569
570 Another notable difference is that Arctic heating is shallower in the CMIP5 and AMIP simulations,
571 with either a relatively weak or no second maxima in heating in the polar stratosphere during the
572 era of AA. There some notable model Arctic sea ice loss studies that simulated a weakened
573 stratospheric polar vortex of comparable magnitude to observed (Kim et al. 2014; Nakamura et al.
574 2015; Zhang et al. 2018). However in many modeling experiments, the simulated weaker
575 stratospheric polar vortex is of sufficiently low amplitude that any dynamically induced cooling is
576 less than any thermodynamic warming forced by sea ice loss (Screen 2017b).
577

578 Consistent with the CMIP5 analysis, the rate of Arctic warming is faster in the observations
579 compared to the NMME suite of models (**Supplementary Figure 7**). In contrast, the rate of
580 warming in the mid-latitudes is much faster in the NMME suite of models relative to the
581 observations (**Figure 4**). Therefore, given that the warming is comparable in both the observations
582 and the NMME ensembles for the entire NH, the models are more equitably distributing heat
583 between the Arctic and the mid-latitudes. However, because some ensemble members simulate
584 warming of the polar vortex and mid-latitude cooling supports that asymmetries between the
585 models and observations are due to natural variability.
586
587 In **Figure B2** we summarize how Arctic amplification influences the mid-latitudes as supported
588 by the majority of model simulations. The large-scale hemispheric circulation is the same pre-AA
589 as shown from the observations with cold air over the Arctic, milder air over the mid-latitudes and
590 subtropics and the stratosphere dominated by a strong polar vortex with higher geopotential heights
591 at lower latitudes. However, in the period of AA, the excess heat generated in the Arctic due to
592 sea ice loss and other mechanisms described above is not redistributed vertically but rather
593 horizontally. The shallower heating does, in many modeling experiments, force a disrupted polar
594 vortex but of comparably weak magnitude. The pre-AA atmospheric circulation and the polar
595 vortex are nearly unchanged in the period of AA other than a weakening of the north to south
596 height gradient between the two periods resulting in no increase in cold air outbreaks from the
597 Arctic to the mid-latitudes in the period of AA. Instead, cold air outbreaks from the Arctic to mid-
598 latitudes are modified, contributing to further warming of the mid-latitudes. Therefore, any
599 induced dynamical cooling is small so that the entire NH warms with the greatest warming
600 occurring over the Arctic.

How then to explain the observed pattern of warm Arctic/cold continents in the era of AA based on the majority modeling experiments? Either natural variability or some other remote forcing is required. Changes in tropical convection have been argued to both amplify Arctic warming (Ding et al. 2014) and disrupt the stratospheric polar vortex (Schwartz and Garfinkle 2017). Therefore, natural variability and/or some remote forcing is responsible for the recent warm Arctic/cold continents pattern more than any contribution from AA.

Methods

In **Figure 1**, air temperature (variable ta) was retrieved from the Earth System Grid Federation (ESGF) archive for the period January 1980 to December 2015 and was averaged on pressure level to obtain a seasonal and zonal mean. A linear trend was then computed at each point in the latitude-pressure plane. The trend was assumed to be distributed according to a t-distribution. For the RCP8.5 scenario of the CMIP5 project, trends were combined by first taking an average over all simulations for each model, then averaging over all models over an institute and then averaged over institutes to obtain a multi-model mean. The distribution of trends at each point in the latitude-pressure plane and for each season was found through bootstrapping with 50,000 samples. For each sample, we randomly select one simulation for each model and then combine all the chosen simulations to obtain a multi-model mean, and then computed a trend using this multi-model mean time series. By repeating this procedure, we obtain a distribution of trends. From this distribution of trends for each season, we can find at each point in the latitude-pressure plane the p-value for the null hypothesis of no trend. We then apply the False Discovery Rate correction (see Wilks 2006) with a global p-value of 0.05. The False Discover Rate correction is a field significance test that calculates a new threshold p-value based on the distribution of p-values. For the reanalyses of the Collaborative REAnalysis Technical Environment – Intercomparison Project, we applied the exact same analysis except that the 50,000 bootstrap samples for the trend distribution were generated in a slightly different fashion. Instead of selecting one simulation for each reanalysis (there is only one), we selected a random trend from each of the reanalyses' trends t-distribution. The linear air temperature trend in **Figure 1c, d** is based on the 16-member Atmosphere Model Intercomparison (AMIP) simulations with the "higher-top" version of the NCAR's Community Atmosphere Model version 5 (CAM5; Richter et al. 2015) for 1980/1981-2015/2016. In **Figure**

632 **1c**, the air temperature is first averaged zonally and seasonally and over all 16 members before the
633 linear trend is calculated. **Figure 1d** is the trend for member #14 that best matches the observation.
634 The air temperature data in AMIP simulations and detailed forcing information are available at:
635 https://www.esrl.noaa.gov/psd/repository/entry/show?entryid=e5555a12-84f8-4bc6-86e3-
636 17b51124c459
637
638 In **Figure 3**, spatial relations among regional and full Arctic 850 hPa air temperature and NH near
639 surface temperatures composited were examined with a series of composites computed with ERA-
640 Interim Reanalysis (Dee et al. 2011). Area-averaged reference means were formed from 1981-
641 2010 in both the near surface temperature and 850 hPa air temperature for the Barents-Kara Sea
642 (65N to 80N, 10E to 100E), west of Greenland (60N to 90N, 80W to 50W), east of Greenland
643 (40W to 10W), and the Chukchi and Bering Sea (65N to 80N, 170E to 210E). The near surface
644 temperature anomalies were regressed onto 850 hPa air temperature using daily data in winter
645 (DJF) 1979/80 to 2016/17; all data is linearly detrended. when the 850 hPa air temperatures were
646 between 0.5 and 3 standard deviations above the climatological average. Completing this analysis
647 is the Polar Cap Temperature at 850 hPa, area-averaged from 65 to 90°N and similarly regressed
648 with NH near surface temperatures (**Figure 3e**). A comparable analysis was completed with
649 HadGEM2 data. The model data is from 1600 winters simulated under present day conditions
650 using the HadGEM2-ES model. Specifically, we ran 400 realizations of five years in length from
651 2008-2012 under the RCP8.5 scenario. Runs were started on Jan. 1st, so there are only four full
652 winters in each five-year run. Initial conditions for the 400 realizations were generated by first
653 branching off 16 different realizations at the year 1990 from historical simulations and then forcing
654 with historical/RCP8.5 forcing until 2008. At year 2008, 25 realizations where branched off of

655 each of the 16 different climate states by using the atmospheric initial conditions from 25 different
656 dates (from Jan. 1st to 25th). Forced response to sea ice in **Figure 3k-o** are from Screen (2017a).

657 In **Figure 4**, the linear trend for December, January, February and March (DJFM) 2-m temperature
658 was computed using both the National Centers for Environmental Prediction (NCEP) Reanalysis
659 (Kalnay et al. 1996) and the November forecast components of the North American Multi-Model
660 Ensemble (NMME, Kirtman et al. 2014). Included in the NMME were models from the Canadian
661 Meteorological Center (CMC1-CanCM3 and CMC2-CanCM4), the Center for Ocean-Land-Air
662 Studies (COLA-RSMAS-CCSM4), and the Geophysical Fluid Dynamics Laboratory (GFDL-
663 CM2p5-FLOR-A06 and GFDL-CM2p5-FLOR-B01). Reference means were computed from
664 1982-2010 for both NCEP and NMME components. For the NMME components, the zero-hour
665 forecasts were treated as analyses for the DJFM period, with each model treated individually; so,
666 for example, the CMC1-CanCM3 analyses for 1982-2010 were used to form the reference mean
667 for computing anomalies in the CMC1-CanCM3 Nov. forecasts for DJFM. For the mid-latitude
668 NH (30 to 60°N), all annual anomalies from 1989-2017 were computed for observed (NCEP) and
669 forecast (NMME Nov. for DJFM), using all ensemble members of the individual NMME
670 components (**Figure 4a** with all in gray, **Figure 4b** with NCEP in blue and NMME in red). The
671 annual mean of all NMME components and ensembles was then used to compute the linear trend
672 computed from 1989-2017 (**Figure 4c** in red) for comparison to the NCEP linear trend (**Figure 4c**
673 in blue). For broader comparison, these calculations were repeated for the entire NH with trend
674 lines for NMME (green) and NCEP (black) shown in **Figure 4d**.

675 In **Supplementary Figure 1a** and **b**, the linear trend is computed for each grid cell in the Hadley
676 Centre-Climate Research Unit CRU global temperature dataset-4 (HadCRUT4; Morice et al. 2012)
677 for land surface only, multiplied by ten to provide a trend in °C/decade for the months October

678 through December and January through March, respectively from 1988-2008. In **Supplementary**
679 **Figure 1c** and **d**, the average surface temperature anomaly is computed for each grid cell in the
680 Hadley Centre CRU land surface data for the months October through December and January
681 through March, respectively from 2008-2018. Climatology used is the thirty-year average of 1981-
682 2010.

683 In **Supplementary Figure 2**, the 2-m air temperature anomalies and the five-year running mean
684 for December through February are plotted for the Arctic, mid-latitudes land areas and the
685 difference between the Arctic and mid-latitudes land areas. Climatology used is the thirty-year
686 average of 1981-2010. Data is from NCEP/NCAR reanalysis data (Kalnay et al. 1996).

687 The simulations presented in **Supplementary Figure 3** and **4** are conducted at NOAA's Earth
688 System Research Laboratory Physical Science Division. These are AMIP simulations from 1979
689 to present day forced by observed GHGs, ozone, aerosols and surface lower boundaries (i.e., sea
690 surface temperature and sea ice conditions). Three model simulations from NCAR "low-top"
691 Community Atmosphere Model Version 5 (30 members; Neale et al. 2012), NCAR "higher-top"
692 CAM5 (16 members; Richter et al. 2015), and ECHAM5 (30 members; Roeckner et al. 2003) are
693 utilized for the decadal temperature trend across 1980-2015.

694 In **Supplementary Figure 3**, the air temperature is first averaged zonally and seasonally and over
695 all available members before the linear trend is assessed. All the data and detailed model
696 simulation information can be found at
697 https://www.esrl.noaa.gov/psd/repository/entry/show?entryid=e5555a12-84f8-4bc6-86e3-
698 17b51124c459
699

In **Supplementary Figure 6**, the linear trend in sea ice concentration from the Hadley Centre Sea Ice and Sea Surface Temperature data set (HadISST; Rayner et al. 2003) are shaded.

In **Supplementary Figure 7**, the winter near surface air temperature anomalies and the linear trend for December, January, February and March (DJFM) was computed using both the NCEP Reanalysis and the November forecast components of the NMME models for the Arctic (60-90°N) and the tropics (0-30°N). Climatology used for reanalysis and NMME is 1981-2010 winter mean from reanalysis.

In **Supplementary Figure 8**, reanalysis is repeated as in **Figure 4** and **Supplementary Figure 5** except that the climatology used is 1981-2010 winter mean from NMME.

Acknowledgements

We are grateful to R. Blackport, C. Deser, L. Sun, J. Screen and D. Smith for many helpful discussions and suggested revisions to the manuscript. We are also grateful for J. Screen and L. Sun for model data. J Cohen is supported by the US National Science Foundation grants AGS-1657748 and PLR-1504361.

Author Contributions

Cohen led the team of authors in writing the text. F. Laliberte created Figure 1. P. Taylor created Figure 2. J. Cohen and K. Pfeiffer created Figure 3. J. Cohen and K. Pfeiffer created Figure 4. J. Cohen created Figures B1 and B2.

Competing Financial Interests

The authors declare no competing financial interests.

References

Alexander, M. A. *et al.* The atmospheric response to realistic Arctic sea-ice anomalies in an AGCM during winter. *J. Climate* **17**, 890–905 (2004).

Alexeev, V. A., Langen, P. L. & Bates, J. R. Polar amplification of surface warming on an aquaplanet in "ghost forcing" experiments without sea ice feedbacks. *Climate Dyn*. **24,** 655–666, https://doi.org/10.1007/s00382-005-0018-3 (2005).

Alexeev, V. A., et al. Vertical structure of recent Arctic warming from observed data and reanalysis products. *Climatic Change* **111**, 215-239, https://doi.org/10.1007/s10584-011-0192-8 (2012).

Ayarzagüena, B. & Screen, J. A. Future Arctic sea-ice loss reduces severity of cold air outbreaks in midlatitudes. *Geophys. Res. Lett*. **43,** 2801–2809, https://doi.org/10.1002/2016GL068092 (2016).

Baldwin, M. P. & Dunkerton, T. J. Stratospheric harbingers of anomalous weather regimes. *Science* **294**, 581–584 (2001).

Basu, S., Zhang, X. & Wang, Z. Eurasian winter storm activity at the end of the century: A CMIP5 multi-model ensemble projection. *Earth's Future*, 6, 61-70, doi:10.1002/2017EF000670 (2018).

Blackport, R. & Kushner, P. J. Isolating the atmospheric circulation response to Arctic sea ice loss in the coupled climate system. *J. Climate* **30**, 2163–2185, https://doi.org/10.1175/JCLI-D-16-0257.1 (2017).

Boe, J., Hall, A. & X. Qu, X. Current GCMs' unrealistic negative feedback in the Arctic. *J. Climate*, **22**, 4682–4695 (2009).

745 Boeke, R. C. & Taylor, P. C. Seasonal energy exchanges in sea ice retreat regions contribute to
746 the inter-model spread in projected Arctic warming. *Nat. Comm*., in review (2018).

747 Boisvert, L. N. & Stroeve, J. C. The Arctic is becoming warmer and wetter as revealed by the
748 Atmospheric Infrared Sounder. *Geophys. Res. Lett*. **42**, 4439–4446,
749 https://doi.org/10.1002/2015GL063775 (2015).

750 Boisvert, L. N., Wu, D. L. & Shie, C.-L. Increasing evaporation amounts seen in the Arctic
751 between 2003 and 2013 from AIRS data. *J. Geophys. Res.* **120,** 6865–6881,
752 https://doi.org/10.1002/2015JD023258 (2015).

753 Charlton-Perez, A. et al. On the lack of stratospheric dynamical variability in low-top versions of
754 the CMIP5 models. *J. Geophys. Res.*, **118**, 2494-2505 doi: https://doi.org/10.1002/jgrd.50125
755 (2013)

756 Chen, H. W., Alley, R. B. & Zhang, F. Interannual Arctic sea ice variability and associated winter
757 weather patterns: A regional perspective for 1979–2014. *J. Geophys. Res. Atmos.* **121**,
758 doi:10.1002/2016JD024769. (2016a).

759 Chen, H. W., Zhang, F. & Alley, R. B. The robustness of midlatitude weather pattern changes due
760 to Arctic sea ice loss. *J. Climate* **29,** 7831–7849, https://doi.org/10.1175/JCLI-D-16-0167.1.
761 (2016b).

762 Chen, X. & Luo, D. Arctic sea ice decline and continental cold anomalies: Upstream and
763 downstream effects of Greenland blocking. *Geophys. Res. Lett*. **44**, 3411–3419,
764 https://doi.org/10.1002/2016GL072387 (2017).

765 Christensen, J. H., Boberg, F., Christensen, O. B. & Lucas-Picher, P. On the need for bias
766 correction of regional climate change projections of temperature and precipitation. *Geophys.*
767 *Res. Lett.* **35,** L20709 (2008).

768 Cohen, J., & Barlow, M. The NAO, the AO, and global warming: How closely related? *J. Climate*
769 **18**, 4498–4513 (2005).

770 Cohen, J., Barlow, M., Kushner, P. J. & Saito, K. Stratosphere-troposphere coupling and links with
771 Eurasian land surface variability. *J. Climate* **20,** 5335–5343,
772 https://doi.org/10.1175/2007JCLI1725.1 (2007).

773 Cohen, J., Barlow, M. & Saito, K. Decadal fluctuations in planetary wave forcing modulate global
774 warming in late boreal winter *J. Climate* **22**, 4418–4426 (2009).

775 Cohen, J., Furtado, J., Barlow, M., Alexeev, V. & Cherry, J. Arctic warming, increasing fall snow
776 cover and widespread boreal winter cooling. *Environ. Res. Lett.* **7**, 014007
777 https://doi.org/10.1088/1748-9326/7/1/014007 (2012a).

778 Cohen, J., Furtado, J., Barlow, M., Alexeev, V. & Cherry, J. Asymmetric seasonal temperature
779 trends. *Geophys. Res. Lett.* **39**, L04705, https://doi.org/10.1029/2011GL050582 (2012b).

780 Cohen, J., Jones, J., Furtado, J. C. & Tziperman, E. Warm Arctic, cold continents: A common
781 pattern related to Arctic sea ice melt, snow advance, and extreme winter weather.
782 *Oceanography* **26**(4), https://doi.org/10.5670/oceanog.2013.70 (2013).

783 Cohen, J. *et al.* Recent Arctic amplification and extreme mid-latitude weather. *Nat. Geosci.* **7,**
784 627–637, https://doi.org/10.1038/ngeo2234 (2014).

785 Cohen, J., *et al.* Arctic change and possible influence on mid-latitude climate and weather. US
786 CLIVAR Report 2018-1, 41pp, doi:10.5065/D6TH8KGW (2018a).

787 Cohen, J., Pfeiffer, K. & Francis, J. Warm Arctic episodes linked with increased frequency of
788 extreme winter weather in the United States. *Nat. Comm.* **9**, https://doi.org/10.1038/s41467-
789 018-02992-9 (2018b).

790 Coumou, D. & Rahmstorf, S. A decade of weather extremes. *Nature Climate Change* **2,** 491–496
791 (2012).

792 Coumou, D., Petoukhov, V., Rahmstorf, S., Petri, S. & Schellnhuber, H. J. Quasi-resonant
793 circulation regimes and hemispheric synchronization of extreme weather in boreal summer.
794 *Proc. Nat. Acad. Sci.* **111,** 12331–12336, https://doi.org/10.1073/pnas.1412797111 (2014).

795 Coumou, D., Lehmann, J. & Beckmann, J. The weakening summer circulation in the Northern
796 Hemisphere mid-latitudes. *Science* **348,** 324–327, https://doi.org/10.1126/science.1261768
797 (2015).

798 Dee, D. P. et al. The ERA-Interim reanalysis: configuration and performance of the data
799 assimilation system. *Q.J.R. Meteorol. Soc.* **137**, 553–597. doi: 10.1002/qj.828 (2011).

800 Deser, C., Walsh, J. E. & Timlin, M. S. Arctic sea ice variability in the context of recent
801 atmospheric circulation trends. *J. Climate* **13**, 617–633 (2000).

802 Deser, C., Magnusdottir, G., Saravanan, R. & Phillips, A. The effects of North Atlantic SST and
803 sea-ice anomalies on the winter circulation in CCM3. Part II: Direct and indirect components
804 of the response. *J. Climate* **17**, 877–889 (2004).

805 Deser, C., Tomas, R. A. & Sun, L. The role of ocean-atmosphere coupling in the zonal-mean
806 atmospheric response to Arctic sea ice loss. *J. Climate* **28,** 2168–2186,
807 https://doi.org/10.1175/JCLI-D-14-00325.1 (2015).

808 *Environ. Res. Lett*. **11,** https://doi.org/10.1088/1748-9326/11/9/094028 (2016).

809 Diffenbaugh, N. S. *et al.* Quantifying the influence of global warming on unprecedented extreme
810 climate events. *Proc. Natl. Acad. Sci. USA*, https://doi.org/10.1073/plans.1618082114 (2017).

811 Ding, Q. *et al.* Tropical forcing of the recent rapid Arctic warming in northeastern Canada and
812 Greenland. *Nature* **509,** 209–212, https://doi.org/10.1038/nature13260 (2014).

813 Ding, Q. *et al.* Influence of high-latitude atmospheric circulation changes on summertime Arctic
814 sea ice. *Nat. Clim. Change* **7** 289–295, https://doi.org/10.1038/NCLIMATE3241 (2017).

815 Döscher, R., Vihma, T. & Maksimovich, E. Recent advances in understanding the Arctic climate
816 system state and change from a sea ice perspective: a review. *Atmos. Chem. Phys*. **14**, 13571-
817 13600, https://doi.org/10.5194/acp-14-13571-2014 (2014).

818 Francis, J. A. & Vavrus, S. J. Evidence linking Arctic amplification to extreme weather in mid-
819 latitudes. *Geophys. Res. Lett.* **39,** https://doi.org/10.1029/2012GL051000 (2012).

820 Francis J. & Vavrus, S. Evidence for a wavier jet stream in response to rapid Arctic warming.
821 *Environ. Res. Lett.* **10,** https://doi.org/10.1088/1748-9326/10/1/014005 (2015).

822 Francis, J. A., Hunter, E., Key, J. R. & Wang, X. Clues to variability in Arctic minimum sea ice
823 extent. *Geophys. Res. Lett.* **32,** https://doi.org/10.1029/2005GL024376 (2005).

824 Gong, T., Feldstein, S. B. & Lee, S. The role of downward infrared radiation in the recent Arctic
825 winter warming trend. *J. Climate,* https://doi.org/10.1175/JCLI-D-16-0180.1 (2017).

826 Gramling, C. Arctic impact. *Science* **347**, 818–821 (2015).

827 Hegyi, B. M., & Taylor P. C. The regional influence of the Arctic Oscillation and Arctic Dipole
828 on the wintertime Arctic surface radiation budget and sea ice growth. *Geophys. Res. Lett.* **44**,
829 4341–4350, doi: 10.1002/2017GL073281 (2017).

Holton, J. R. *An Introduction to Dynamic Meteorology, Second Edition.* Academic Press, New York, 416 pp. (1979).

Honda, M., Inoue, J. & Yamane, S. Influence of low Arctic sea-ice minima on anomalously cold Eurasian winters. *Geophys. Res. Lett.* **36,** https://doi.org/10.1029/2008GL037079 (2009).

Huang, J., Zhang, X., Zhang, Q., Lin, Y., Hao, M., Luo, Y., Zhao, Z., Yao, Y., Chen, X., Wang, L., Nie, S., Yin, Y., Xu, Y. & Zhang, J. Recently amplified Arctic warming has contributed to a continual global warming trend. *Nat. Clim. Change* **7**, 875–880, doi:10.1038/s41558-017-0009-5 (2017).

Intrieri, J. M. *et al.* An annual cycle of Arctic surface cloud forcing at SHEBA. *J. Geophys. Res*. **107,** https://doi.org/10.1029/2000JC000423 (2002).

IPCC. Summary for Policymakers. In: *Climate Change 2013: The Physical Science Basis. Contribution of Working Group I to the Fifth Assessment Report of the Intergovernmental Panel on Climate Change* [Stocker, T.F., D. Qin, G.-K. Plattner, M. Tignor, S. K. Allen, J. Boschung, A. Nauels, Y. Xia, V. Bex and P.M. Midgley (eds.)]. Cambridge University Press, Cambridge, United Kingdom and New York, NY, USA (2013).

Jaiser, R., Dethloff, K., Handorf, D., Rinke, A. & Cohen, J. Impact of sea ice cover changes on the Northern Hemisphere atmospheric winter circulation. *Tellus A* **64,** https://doi.org/10.3402/tellusa.v64i0.11595 (2012).

Jaiser, R. *et al.* Atmospheric winter response to Arctic sea ice changes in reanalysis data and model simulations. *J. Geophys. Res.* **121,** 7564–7577, https://doi.org/10.1002/2015JD024679 (2016).

Jeong, J.-H. *et al.* Intensified Arctic warming under greenhouse warming by vegetation–atmosphere–sea ice interaction. *Env. Res. Lett*. **9**, 094007 (2014).

852 Johnson, N. C., Xie, S.-P., Kosaka, Y. & Li, X. Increasing occurrence of cold and warm extremes
853 during the recent global warming slowdown. *Nat. Comm.* **9**, https://doi.org/10.1038/s41467-
854 018-04040-y (2018).

855 Kalnay, E. *et al.* The NCEP/NCAR 40-year reanalysis project. *Bull. Amer. Meteor. Soc.* **77**, 437–
856 471 (1996).

857 Kay, J. E. & L'Ecuyer, T. Observational constraints on Arctic ocean clouds and radiative fluxes
858 during the early 21st century. *J. Geophys. Res. Atmos.* **118,** 7219–7236,
859 https://doi.org/10.1002/jgrd.50489 (2013).

860 Kim, B.-M. *et al.* Weakening of the stratospheric polar vortex by Arctic sea-ice loss. *Nat. Comm.*
861 **5,** https://doi.org/10.1038/ncomms5646 (2014).

862 Kintisch, E. Into the maelstrom. *Science* **344,** 250–253 (2014).

863 Kirtman, B. P. e*t al.* The North American Multimodel Ensemble. *Bull. Am. Meteorol. Soc*. **17**,
864 585–601, https://doi.org/10.1175/BAMS-D-12-00050.1 (2014).

865 Kretschmer, M. *et al.* More frequent weak stratospheric polar vortex states linked to mid-latitude
866 cold extremes. *Bull. Am. Meteorol. Soc*., https://doi.org/10.1175/BAMS-D-16-0259.1 (2018).

867 Kug, J.-S. *et al.* Two distinct influences of Arctic warming on cold winters over North America
868 and East Asia. *Nat. Geosci.* **8,** 759–762, https://doi.org/10.1038/ngeo2517 (2015).

869 Kvamsto, N. G., Skeie P. & Stephenson, D. B. Impact of Labrador sea-ice extent on the North
870 Atlantic Oscillation. *Int. J. Climatol.* **24**, 603–612 (2004).

871 Laliberte, F. & Kushner, P. J. Midlatitude moisture contribution to recent Arctic tropospheric
872 summertime variability. *J. Climate* **27,** 5693–5706, https://doi.org/10.1175/JCLI-D-13-
873 00721.1 (2014).

874 Lee, S. A theory for polar amplification from a general circulation perspective. *Asia-Pac. J. Atmos.*
875 *Sci*. **50,** 31–43, https://doi.org/10.1007/s13143-014-0024-7 (2014).

876 Lehmann, J., Coumou, D. & Frieler, K. *Climatic Change* **132**, https://doi.org/10.1007/s10584-015-
877 1434-y (2015).

878 Liu, Y. & Key, J. R. Less winter cloud aids summer 2013 Arctic sea ice return from 2012
879 minimum. *Environ. Res. Lett*. **9,** https://doi.org/10.1088/1748-9326/9/4/044002 (2014).

880 Magnusdottir, G., Deser, C. & Saravanan, R. The effects of North Atlantic SST and sea-ice
881 anomalies on the winter circulation in CCM3. Part I: Main features and storm track
882 characteristics of the response. *J. Climate* **17**, 857–876 (2004).

883 Manabe, S. & Wetherald, R. T. The effects of doubling the CO_2 concentration on the climate of a
884 general circulation model. *J. Atmos. Sci.* **32,** 3–15, https://doi.org/10.1175/1520-
885 0469(1975)032<0003:TEODTC>2.0.CO;2 (1975).

886 Martius, O., Polvani, L. M. & Davie, H. C. Blocking precursors to stratospheric sudden warming
887 events. *Geophys. Res. Lett.* **36**, L14806 (2009).

888 McCusker, K. E., Fyfe, J. C. & Sigmond, M. Twenty-five winters of unexpected Eurasian cooling
889 unlikely due to Arctic sea ice loss. *Nat. Geosci*. **9,** 838–842, https://doi.org/10.1038/ngeo2820
890 (2016).

891 Melillo, J. M., Richmond, T. C. & Yohe, G. W. Climate Change Impacts in the United States: The
892 Third National Climate Assessment, https://doi.org/10.7930/J0Z31WJ2 (2014).

893 Min, E., Hazeleger, W., Odenborgh, G. J. & Sterl, A. Evaluation of trends in high temperature
894 extremes in north-western Europe in regional climate models. *Env. Res. Lett.* **8**, 014011
895 https://doi.org/10.1088/1748-9326/8/1/014011 (2013).

Mori, M., Watanabe, M., Shiogama, H., Inoue, J. & Kimoto, M. Robust Arctic sea-ice influence on the frequent Eurasian cold winters in past decades. *Nat. Geosci.* **7,** 869–873, https://doi.org/10.1038/ngeo2277 (2014).

Morice, C. P., Kennedy, J. J., Rayner, N. A. & Jones, P. D. Quantifying uncertainties in global and regional temperature change using an ensemble of observational estimates: the HadCRUT4 dataset. *Journal of Geophysical Research* **117**, D08101, doi:10.1029/2011JD017187 (2012).

Munich Re. Severe weather in North America. Knowledge Series: Natural Hazards, https://www.munichre.com/us/property-casualty/knowledge/expertise/knowledge-publications/severe-weather/index.html (2012).

Mysak, L. A. & Venegas, S. A. Decadal climate oscillations in the Arctic: A new feedback loop for atmosphere-ice-ocean interactions. *Geophys. Res. Lett.* **25**, 3607–3610 (1998).

Nakamura, T. *et al.* A negative phase shift of the winter AO/NAO due to the recent Arctic sea-ice reduction in late autumn. *J. Geophys. Res.* **120,** 3209–3227, https://doi.org/10.1002/2014JD022848 (2015).

National Academies of Sciences, Engineering, and Medicine. Attribution of Extreme Weather Events in the Context of Climate Change. Washington, DC: The National Academies Press. doi: 10.17226/21852 (2016).

Neale R. B., *et al*. Description of the NCAR Community Atmosphere Model (CAM 5.0), NCAR Technical Note NCAR TN 486 (2012).

Newson, R. L. Response of a general circulation model of the atmosphere to removal of the Arctic ice-cap. *Nature* **241**, 39-40 (1973).

Ogawa, F. *et al*. Evaluating impacts of recent Arctic sea ice loss on the northern hemisphere winter climate change. *Geophys. Res. Lett.* **45**, 3255–3263, https://doi.org/10.1002/2017GL076502 (2018).

Orsolini, Y., Senan, R., Benestad, R. E. & Melsom, A. Autumn atmospheric response to the 2007 low Arctic sea ice extent in coupled ocean-atmosphere hindcasts. *Climate Dyn.* **38,** 2437–2448 https://doi.org/10.1007/s00382-011-1169-z (2012).

Overland, J. E. & Wang, M. Large-scale atmospheric circulation changes are associated with the recent loss of Arctic sea ice. *Tellus* **62A**, 1–9, https://doi.org/10.1111/j.1600-0870.2009.00421.x (2010).

Overland, J. E., Wood, K. R. & Wang, M. Warm Arctic–cold continents: Impacts of the newly open Arctic Sea. *Polar Res.* **30,** 15787 (2011).

Overland, J. E., Francis, J. A., Hanna, E. & Wang, M. The recent shift in early summer Arctic atmospheric circulation. *Geophys. Res. Lett.* **39,** L19804, https://doi.org/10.1029/2012GL053268 (2012).

Overland, J. E. *et al.* The melting Arctic and mid-latitude weather patterns: Are they connected? *J. Climate* **28,** 7917–7932, https://doi.org/10.1175/JCLI-D-14-00822.1 (2015).

Overland, J. E. *et al.* Nonlinear response of mid-latitude weather to the changing Arctic. *Nature Climate Change* **6,** 992–999, https://doi.org/10.1038/NCLIMATE3121 (2016).

Park, D.-S., Lee, S. & Feldstein, S. B. Attribution of the recent winter sea-ice decline over the Atlantic sector of the Arctic Ocean. *J. Climate* **28**, 4027–4033, https://doi.org/10.1175/JCLI-D-15-0042.1 (2015).

938 Park, H.-S., Lee, S., Kosaka, Y., Son, S.-W. & Kim, S.-W. The impact of Arctic winter infrared
939 radiation on early summer sea ice. *J. Climate* **28**, 6281–6296, https://doi.org/10.1175/JCLI-D-
940 14-00773.1 (2015).

941 Perovich, D. K., Richter-Menge, J. A., Jones, K. F. & Light, B. Sunlight, water, and ice: Extreme
942 Arctic sea ice melt during the summer of 2007. *Geophys. Res. Lett.* **35,**
943 https://doi.org/10.1029/2008gl034007 (2008).

944 Pistone, K., Eisenman, I. & Ramanathan, V. Observational determination of albedo decrease
945 caused by vanishing Arctic sea ice. *Proc. Nat. Acad. Sci.* **111,** 3322–3326,
946 https://doi.org/10.1073/pnas.1318201111 (2014).

947 Pithan, F. & Mauritsen, T. Arctic amplification dominated by temperature feedbacks in
948 contemporary climate models. *Nature Geosci.* **7**, 181–184 (2014).

949 Quiroz, R. S. Tropospheric-stratospheric interaction in the major warming event of January-
950 February 1979. *Geophys. Res. Lett.* **6**, 6451–648 (1979).

951 Quiroz, R. S. The association of stratospheric warmings with tropospheric blocking. *J. Geophys.*
952 *Res.* **91**, 52771–5285 (1986).

953 Rahmstorf, S. & Coumou, D. Increase of extreme events in a warming world. *Proc. Natl. Acad.*
954 *Sci. USA* **108**, 17905–17909, https://doi.org/10.1073/pnas.1101766108 (2011).

955 Rayner, N. A., Parker, D. E., Horton, E. B., Folland, C. K., Alexander, L. V. Rowell, D. P., Kent,
956 E. C., & Kaplan, A. Global analyses of sea surface temperature, sea ice, and night marine air
957 temperature since the late nineteenth century. *J. Geophys. Res.* **108**, 4407
958 10.1029/2002JD002670 (2003).

959 Rex, D. F. Blocking action in the middle troposphere and its effect upon regional climate I. An
960 aerological study of blocking action. *Tellus* **2**, 1961–211 (1950a).

961 Rex, D. P. Blocking action in the middle troposphere and its effect upon regional climate (II). The
962 climatology of blocking actions. *Tellus* **2**, 2751–301 (1950b).

963 Richter J., Deser, C. & Sun, L. Effects of stratospheric variability on El Niño teleconnections.
964 *Environ. Res. Lett.* **10**, 124021 (2015).

965 Rigor, I. G., Wallace, M. & Colony, R. Response of sea ice to the Arctic Oscillation. *J.*
966 *Climate*, **15,** 2648–2663 (2002).

967 Roeckner, E., *et al.* The atmospheric general circulation model ECHAM5. Part I: Model
968 description, Max Planck Institute for Meteorology Tech. Rep. 349, 127 pp (2003).

969 Schwartz, C. & Garfinkel, C.I. Relative Roles of the MJO and Stratospheric Variability in North
970 Atlantic and European Winter Climate. *J. Geophys. Res*. **44**, doi:10.1002/2016JD025829
971 (2017).

972 Screen, J. A. Simulated atmospheric response to regional and Pan-Arctic sea-ice loss. *J. Climate,*
973 **30**, https://doi.org/10.1175/JCLI-D-16-0197.1 (2017a).

974 Screen, J. A. The missing Northern European cooling response to Arctic sea ice loss. *Nat.*
975 *Commun*. **8**, 14603 (2017b).

976 Screen, J. A. & Simmonds, I. The central role of diminishing sea ice in recent Arctic temperature
977 amplification. *Nature* **464,** 1334–1337, https://doi.org/10.1038/nature09051 (2010).

978 Screen J. A., Deser, C., Simmonds, I. & Tomas, R. Atmospheric impacts of Arctic sea-ice loss,
979 1979-2009: Separating forced change from atmospheric internal variability. *Climate Dyn.* **43,**
980 333–344, https://doi.org/10.1007/s00382-013-1830-9 (2014).

981 Screen, J. A. *et al.* Consistency and discrepancy in the atmospheric response to Arctic sea-ice loss
982 across climate models. *Nat. Geoscience* **11**(3), 155–163, https://doi.org/10.1038/s41561-018-
983 0059-y (2018).

984 Semmler, T. *et al.* Seasonal atmospheric responses to reduced Arctic sea ice in an ensemble of
985 coupled model simulations. *J. Climate* **29,** 5893–5913, https://doi.org/10.1175/JCLI-D-15-
986 0586.1 (2016).

987 Serreze, M. C. & Francis, J. A. The arctic amplification debate. *Climatic Change* **76**(3–4), 241–
988 264, https://doi.org/1007/s10584-005-9017-y (2006).

989 Shepherd, T. G. Effects of Arctic warming. *Science* **353** 989–990,
990 https://doi.org/10.1126/science.aag2349 (2016).

991 Sillmann, J., Croci-Maspoli, M. Kallache, M. & Katz, R. W. Extreme cold winter temperatures in
992 Europe under the influence of North Atlantic atmospheric blocking. *J. Climate* **24**, 5899–5913
993 (2011).

994 Sillmann, J., Kharin, V. V., Zwiers, F. W., Zhang, X. & Bronaugh, D. Climate extreme indices in
995 the CMIP5 multi-model ensemble. Part 2: Future climate projections. *J. Geophys. Res.* **118**,
996 2473–2493 (2013).

997 Singarayer, J. S., Valdes P. J. & Bamber, J. L. The atmospheric impact of uncertainties in recent
998 Arctic sea-ice reconstructions. *J. Climate* **18**, 3996–4012 (2005).

999 Smith, D. M. *et al.* Atmospheric response to Arctic and Antarctic sea ice: the importance of ocean-
1000 atmosphere coupling and the background state. *J. Climate* **30**(12)
1001 https://doi.org/10.1175/JCLI-D-16-0564.1 (2017).

1002 Smith, D. M. *et al*. The Polar Amplification Model Intercomparison Project (PAMIP) contribution
1003 to CMIP6: investigating the causes and consequences of polar amplification. *Geosci. Model*
1004 *Dev.,* submitted (2018).

1005 Smith, K., Kushner P. J. & Cohen, J. The role of linear interference in Northern Annular Mode
1006 variability associated with Eurasian snow cover extent. *J. Climate* **24**, 6185–6202 (2011).

1007 Stroeve, J. C. *et al.* Trends in Arctic sea ice extent from CMIP5, CMIP3 and observations.
1008 *Geophys. Res. Lett.* **39,** https://doi.org/10.1029/2012GL052676 (2012).

1009 Sun, L., Deser, C. & Tomas, R. A. Mechanisms of stratospheric and tropospheric circulation
1010 response to projected Arctic sea ice loss. *J. Climate* **28,** 7824–7845,
1011 https://doi.org/10.1175/JCLI-D-15-0169.1 (2015).

1012 Sun, L., Perlwitz, J. & Hoerling, M. What caused the recent "Warm Arctic, Cold Continents" trend
1013 pattern in winter temperatures? *Geophys. Res. Lett.* **43,** 5345–5352 (2016).

1014 Taylor, P. C., Maslowski, W. Perlwitz, J. & Wuebbles, D. J. Arctic Changes and their Effects on
1015 Alaska and the Rest of the United States. In: *Climate Science Special Report: Fourth National*
1016 *Climate Assessment, Volume I* [Wuebbles, D. J., S. W. Fahey, K. A. Hibbard, D. J. Dokken,
1017 B. C. Steward, and T. K. Maycock (eds.)]. U.S. Global Climate Change Research Program,
1018 Washington, DC, USA, pp. 303-332, doi: 10.7930/J00863GK (2017).

1019 Taylor, P. C., Hegyi, B. M., Boeke, R. C. & Boisvert, L. N. On the increasing importance of air-
1020 sea exchanges in a thawing Arctic: A review. *Atmos.* **9**, https://doi.org/10.3390/atmos9020041
1021 (2018).

1022 Thompson, D. W. J. & Wallace, J. M. Regional climate impacts of the northern hemisphere annular
1023 mode. *Science* **293**, 85–89, https://doi.org/10.1126/science.1058958 (2001).

1024 Uttal, T. *et al.* Surface heat budget of the Arctic Ocean. *Bull. Amer. Meteor. Soc.* **83,** 255–275,
1025 https://doi.org/10.1175/1520-0477(2002)083<0255:SHBOTA>2.3.CO;2 (2002).

1026 Vihma, T. Effects of Arctic sea ice decline on weather and climate: a review. *Surveys in Geophys.,*
1027 https://doi.org/10.1007/s10712-014-9284-0 (2014).

1028 Vihma, T. Weather Extremes Linked to Interaction of the Arctic and Midlatitudes in Wang, S.-Y.
1029 S., In Yoon, J.-H., In Funk, C. C., & In Gillies, R. R. *Climate extremes: Patterns and*
1030 *mechanisms*. AGU Geophysical Monograph Series, 226 (2017).

1031 Wallace, J. M., Held, I. M., Thompson, D. W. J., Trenberth, K. E. & Walsh, J. E. Global warming
1032 and winter weather. *Science* **343**, 729–730, https://doi.org/10.1126/science.343.6172.729
1033 (2014).

1034 Wang, J. & Ikeda, M. Arctic oscillation and Arctic sea-ice oscillation. *Geophys. Res. Lett.* **27**(9),
1035 1287–1290 (2000).

1036 Wang, J., Ikeda, M., Zhang S. & Gerdes, R. Linking the Northern Hemisphere sea-ice reduction
1037 trend and the quasi-decadal Arctic sea-ice oscillation. *Climate Dyn.* **24**, 115–130 (2005).

1038 Warshaw, M., & Rapp, R. R. An experiment on the sensitivity of a global circulation model. *J.*
1039 *Appl. Meteor*. **12**, 43-49 (1973).

1040 Wegmann, M., Orsolini, Y. J. & Zolina, O. Warm Arctic–cold Siberia: comparing the recent and
1041 the early 20th century Arctic warmings. *Environ. Res. Lett.* **13**, https://doi.org/10.1088/1748-
1042 9326/aaa0b7 (2017).

1043 Wendisch, M. *et al.* Understanding causes and effects of rapid warming in the Arctic. *Eos* **98,**
1044 https://doi.org/10.1029/2017EO064803 (2017).

1045 Wilks, D. *Statistical methods in the atmospheric sciences.* Academic Press, San Diego, California,
1046 464 pp., ISBN:9780123850225 (2006).

1047 Yao, Y., Luo, D., Dai, A. & Simmonds, I. Increased quasi stationarity and persistence of Ural
1048 blocking and Eurasian extreme cold events in response to Arctic warming. Part I: Insights from
1049 observational analyses. *J. Climate* **30,** 3549–3568, https://doi.org/10.1175/JCLI-D-16-0261.1
1050 (2017).

1051 Zhang, P., Wu, Y., Simpson, I. R., Smith, K. L., Zhang, X., De, B. & Callaghan, P. A stratospheric
1052 pathway linking a colder Siberia to Barents-Kara sea ice loss. *Sci. Adv.* **4**, eaat6025 (2018).

1053 Zhang, X., Ikeda, M. & Walsh, J. E. Arctic sea-ice and freshwater changes driven by the
1054 atmospheric leading mode in a coupled sea ice-ocean model. *J. Clim.* **16**, 2159–2177 (2003).

1055 Zhang, X., Sorteberg, A., Zhang, J., Gerdes, R. & Comiso, J. C. Recent radical shifts in
1056 atmospheric circulations and rapid changes in Arctic climate system. *Geophys. Res. Lett.* **35**,
1057 L22701, doi:10.1029/2008GL035607 (2008).

1058 Zhang, X., Lu, C. & Guan, Z. Weakened cyclones, intensified anticyclones, and the recent extreme
1059 cold winter weather events in Eurasia. *Environ. Res. Lett.* **7**, 044044, doi:10.1088/1748-
1060 9326/7/4/044044 (2012).

1061 Zhang, X., He, J., Zhang, J., Polaykov, I., Gerdes, R., Inoue, J. & Wu, P. Enhanced poleward
1062 moisture transport and amplified the northern high-latitude wetting trend. *Nature Clim. Change*
1063 **3**, 47–51, doi: 10.1038/nclimate1631 (2013).

1064

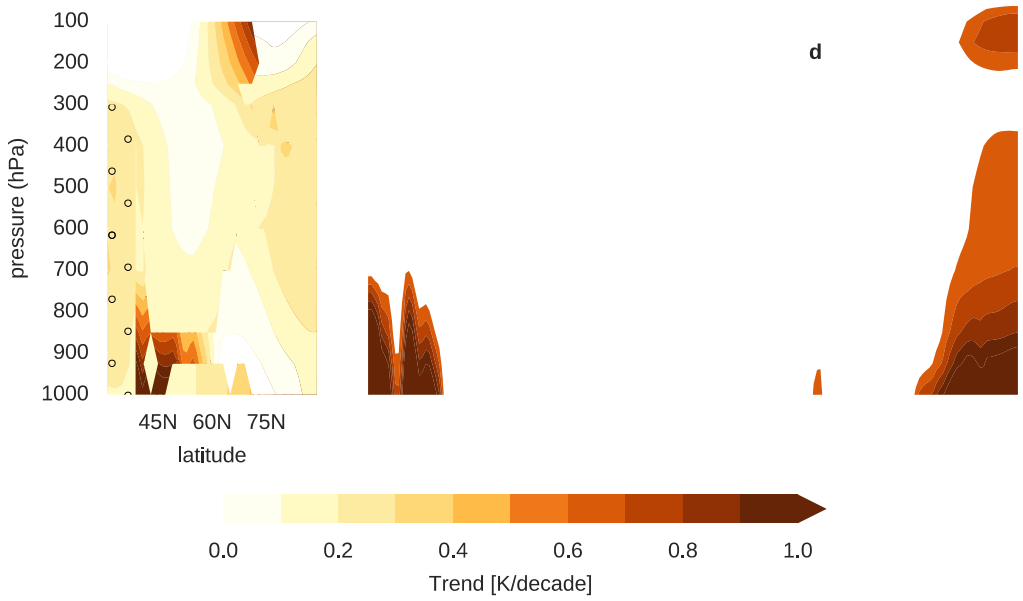

Figure 1. **Observed and ensemble mean temperature trends show large discrepancies in winter**. **a** Seasonal and zonal-mean air temperature trends from 1980-2015 for the average of the MERRA, MERRA-2, ERA-Interim, JRA-55 and CFSR reanalysis products for DJF. **b** Same as **a** but for the CMIP5 multi-model mean historical + RCP8.5. **c** Same as **a** but for the AMIP multi-model mean. **d** Same as **c** but for the AMIP ensemble member that best matches the reanalysis mean. Stippling indicates trends significant with a $p < 0.05$ after the false discovery rate was applied (Wilks 2006).

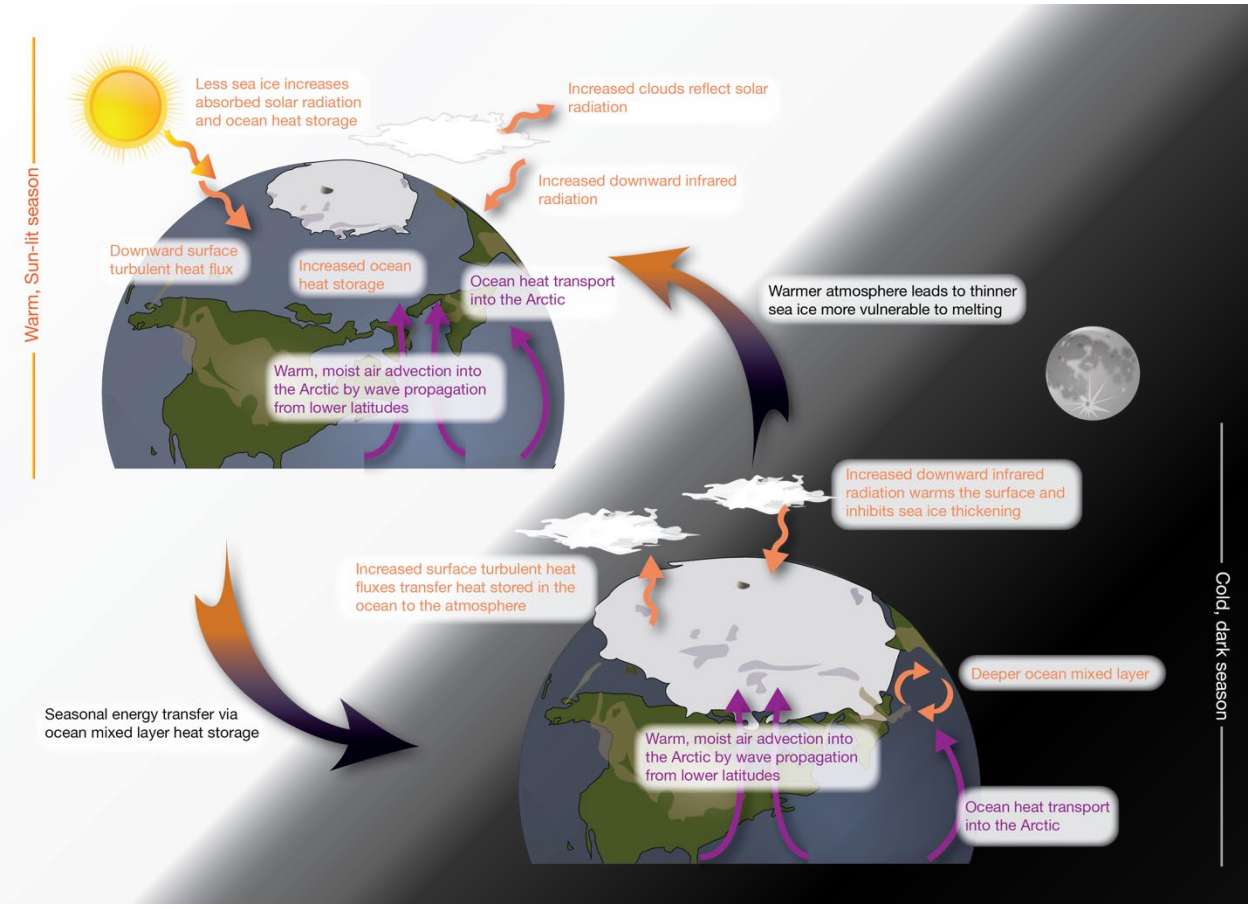

1075

1076 **Figure 2**. **Mechanisms for Arctic amplification are complicated**. Schematic illustrates the
1077 important processes and energy flows influencing Arctic amplification. Local processes, such as
1078 the sea ice albedo feedbacks, surface turbulent fluxes, clouds, ocean heat storage, and ocean mixed
1079 layer change are highlighted in peach. Remote processes, such as atmosphere and ocean heat
1080 transport are highlighted in purple. An important aspect of Arctic amplification is the seasonal
1081 transfer of energy from sun-lit to the dark season denoted by the graduated arrow (orange-black).

1082
1083

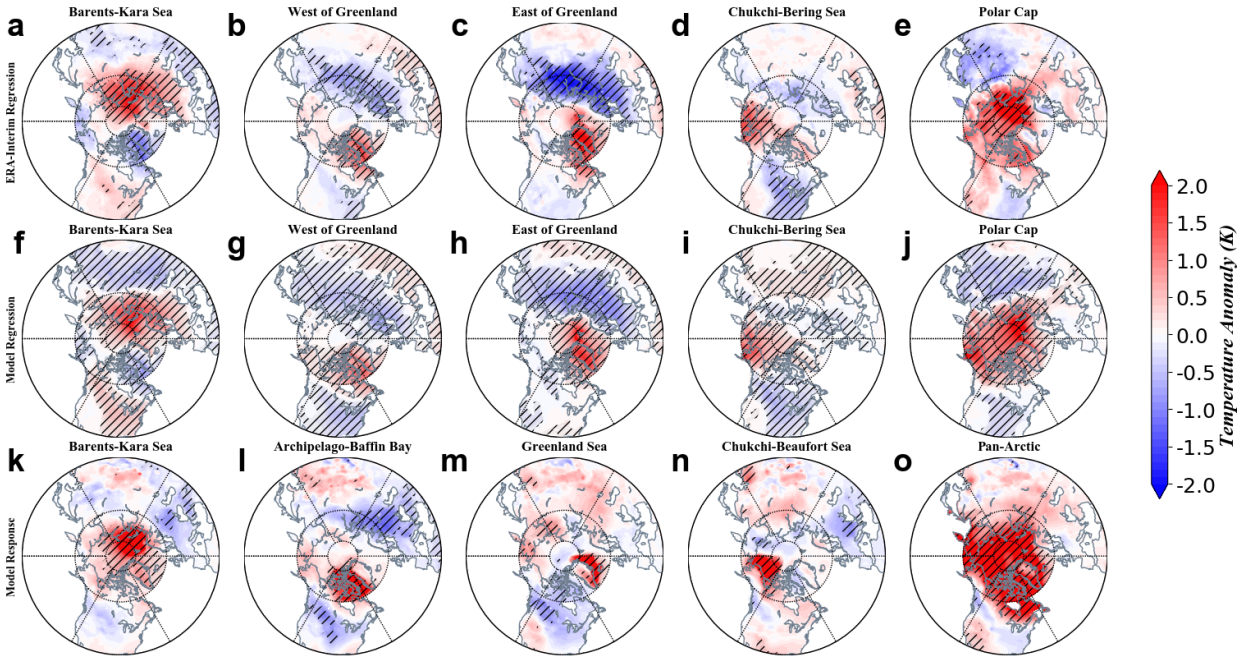

1084

1085 **Figure 3. Observed and simulated temperature relationships to Arctic warming share**
1086 **similarities regionally.** Northern Hemisphere near-surface air temperature anomalies for all days
1087 when 850 hPa temperature anomalies were between 0.5 and 3.0 standard deviations above the
1088 climatological average for all winters (DJF) 1950-2016 for **a** Barents-Kara Seas, **b** Greenland Sea,
1089 **c** Labrador Sea, **d** Chukchi-Bering Seas, and **e** Pan-Arctic regressed onto NH surface
1090 temperatures. Climatological averages computed over the period 1981-2010. **f-j** same as for **a-e**
1091 but for the HadGEM2 GCM. October-to-March mean near-surface air temperature responses in
1092 HadGEM2 model simulations from Screen (2017) to observed sea-ice loss in the **k** Barents-Kara
1093 Sea, **l** Archipelago-Baffin Bay, **m** Greenland Sea, **n** Beaufort-Chukchi Sea, and **o** Pan Arctic.
1094 Hashing denotes statistically significant response at the 95% confidence level.

1095

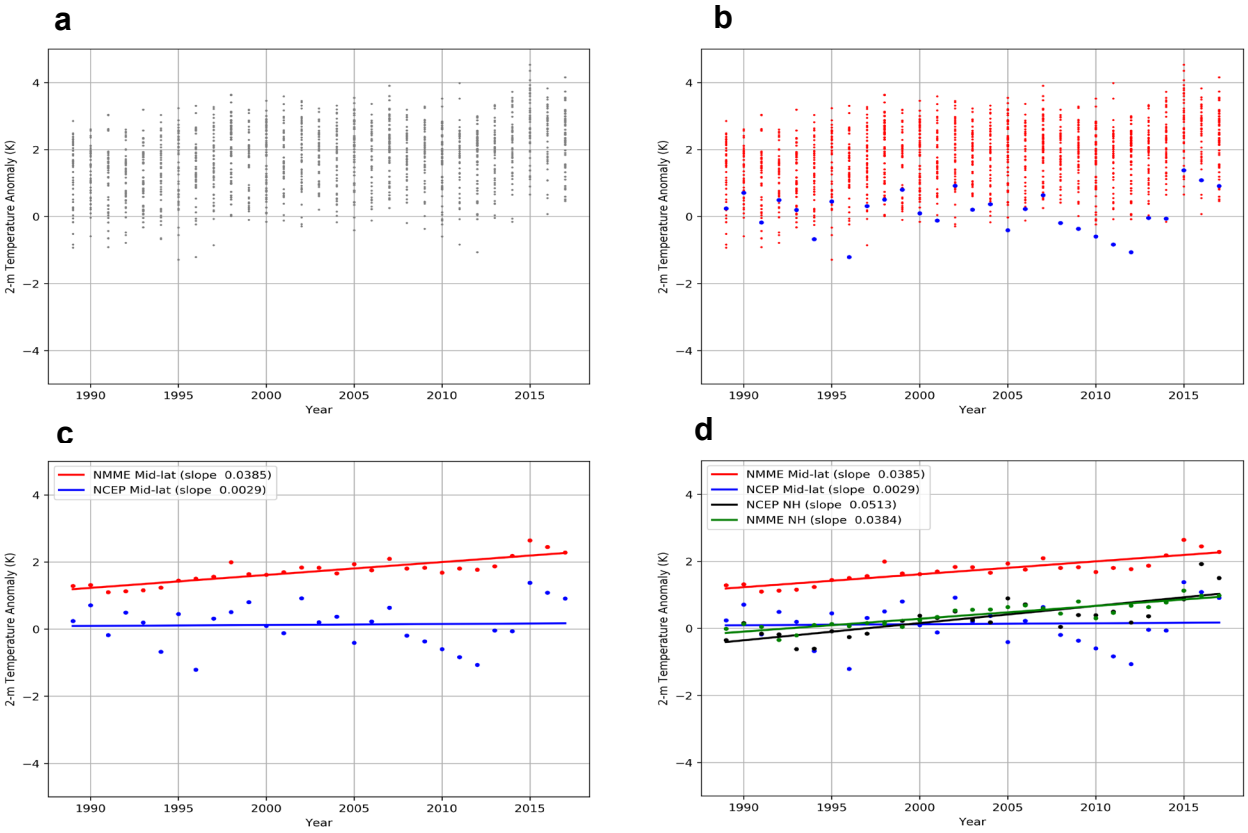

Figure 4. Observed and simulated mid-latitude temperature trends are diverging. **a** Reanalysis and hindcasted/predicted mid-latitude continental temperature anomalies from NMME ensemble members for December, January, February and March from 1988 through 2018. **b** same as **a** but reanalysis plotted in blue and NMME plotted in red. **c** Reanalysis and hindcasted/predicted mid-latitude continental temperature anomalies from NMME ensemble mean for December, January, February and March from 1988 through 2018. Also included is the linear trend line for each dataset. **d** Same as **c** including reanalysis and hindcasted/predicted Northern Hemisphere temperature anomalies from reanalysis (black) and NMME (green) for December, January, February and March from 1988 through 2018 and linear trends. Climatology used for reanalysis and NMME is 1981-2010 winter mean from reanalysis.

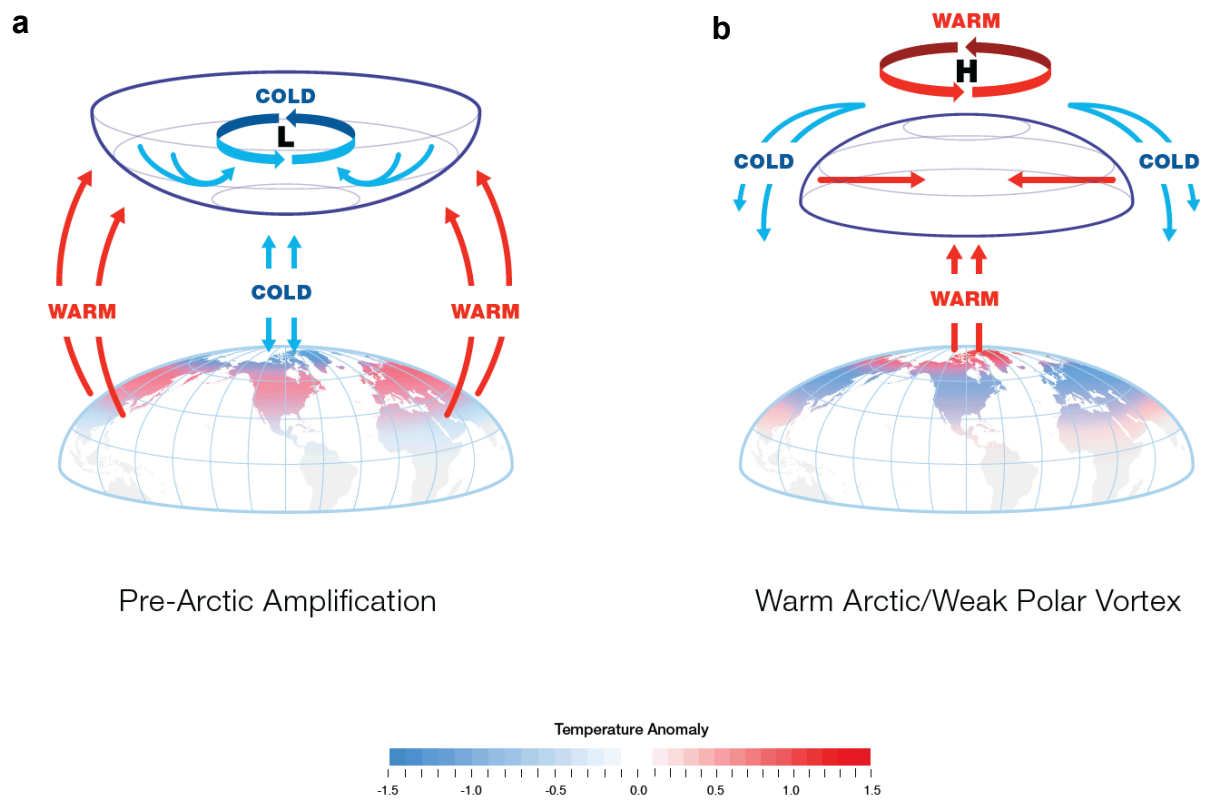

Figure B1. **Schematic of stratospheric polar vortex and resultant temperature anomalies pre and during Arctic amplification based on observational studies**. **a** Climatology favors a strong polar vortex supported by cold air over the Arctic and milder air at lower latitudes. This temperature distribution favors low heights over the Arctic and higher heights in the mid-latitudes. **b** However, during the period of Arctic amplification, excess heating near the Arctic surface is distributed vertically, leading to more high latitude blocking that favors more frequent intrusions of warm air from lower latitudes into the polar stratosphere while cold air is displaced to lower latitudes. This results in an inversion of the circulation pattern in the polar stratosphere with high heights over the Arctic and lower heights in the mid-latitudes.

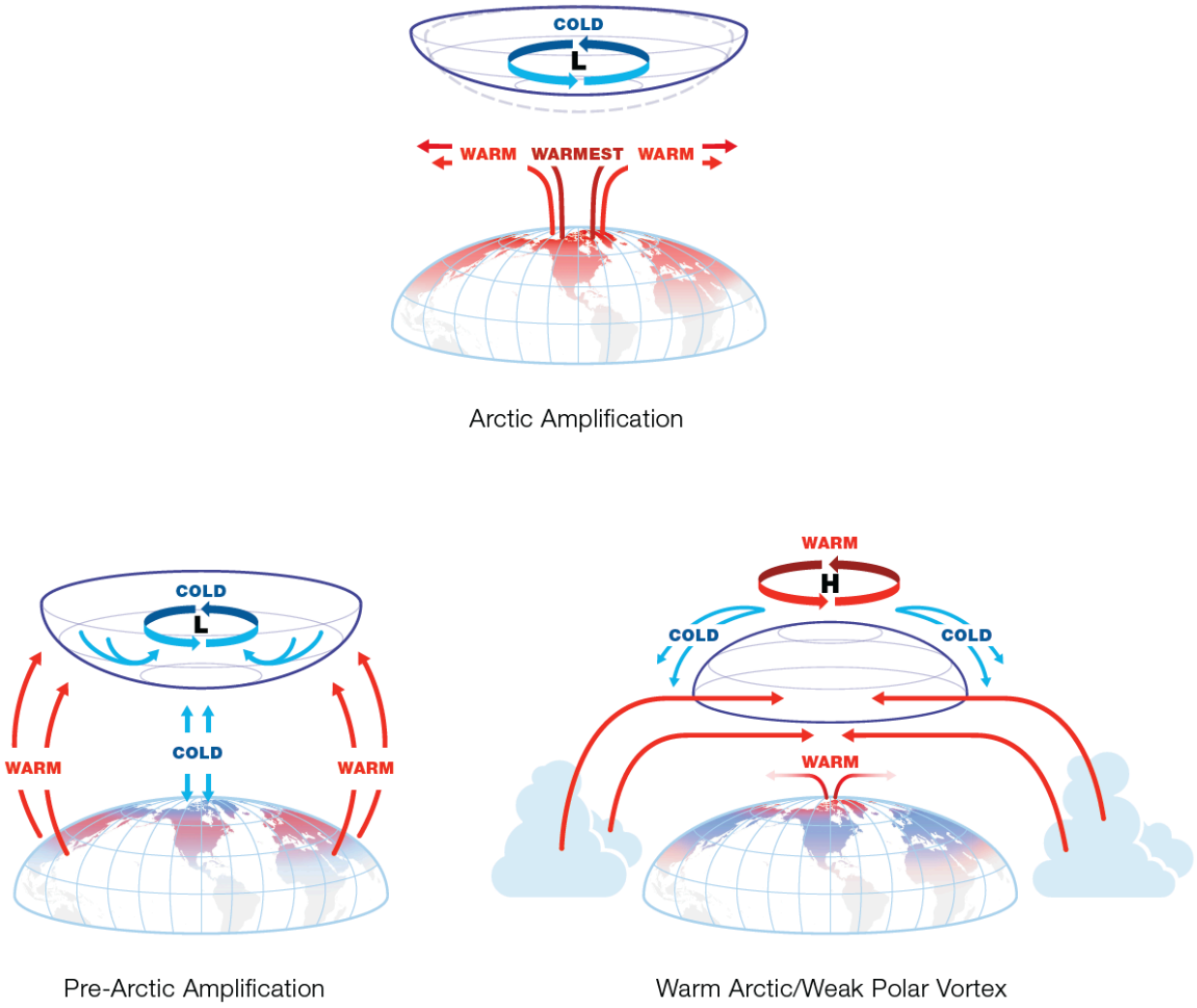

Figure B2. Schematic of stratospheric polar vortex and resultant temperature anomalies pre and during Arctic amplification based on modeling studies. Conceptual mechanisms shown derived from archived ensembles coordinated among modeling centers. **a** Most model experiments support that Arctic amplification disrupts the polar vortex but of weak amplitude. Any induced cooling due to changes in the polar vortex are overwhelmed by warming of the Arctic and transport of the milder Arctic air southward. **b** Same as Figure B1a. However, during the

period of Arctic amplification, observed colder temperatures in the mid-latitudes is due to natural or internal variability. **c** For example, changes in tropical convection transports additional heat both into the Arctic, resulting in amplified Arctic warming, and into the polar stratosphere leading to a more amplified disruption of the polar vortex and displacement of cold air southwards to lower latitudes. Dynamic cooling offsets any thermodynamic warming forced by Arctic amplification.